Observatory of the dynamics of interactions between societies and environment in the amazon

Grant Agreement No. 691053

Deliverable D3.3: "Socio-environmental indicators with demonstrators built on a few selected sites"

WP3:

"ENVIRONMENTAL DYNAMICS:

OBSERVATION & UNDERSTANDING"

Due by: 09/01/2018

Delivery Date of first report: 26/09/2018

Dissemination Level: Public (PU)

Project funded by the European Commission under the Marie Skłodowska-Curie Actions programme within theResearch and Innovation Staff Exchange (RISE) Call: H2020-MSCA-RISE-2015

Project Reference	691053		
Acronym	ODYSSEA		
Project Title	Observatory of the dynamics of interactions between societies and environment in the amazon		
Project URL	www.odyssea-amazonia.org		
Authors (Partner)	Damien Arvor (CNRS, UR2), Pierre Couteron (IRD), Lilian Blanc (CIRAD), Ana Cabral (ISA), Marie-Paule Bonnet (IRD), Emmanuel Roux (IRD), Vincent Dubreuil (UR2), Christovam Barcellos (FIOCRUZ)		
Contact	Damien Arvor, *WP3 Leader* Marie-Paule Bonnet, *project coordinator*	**E-mail**	damien.arvor@univ-rennes2.fr marie-paule.bonnet@ird.fr

Socio-environmental indicators with demonstrators built on a few selected sites

WP3

Environmental dynamics: observation and understanding

Abstract

This deliverable has been written by the WP3 team of the ODYSSEA project. It introduces the main environmental indicators produced on various study areas across the Brazilian Amazon. These indicators provide information on the land cover dynamics in forested and agricultural areas. It also give indication on the evolution of hydrological resources and climate change. In addition, some of these indicators are crossed with socio-economic data to compute socio-environmental indicators with the objective to better understand the interrelationships between local societies and their environment. These socio-environmental indicators focus on the link between deforestation and economic development, health-environment studies, agricultural development and climate, and climate change perceptions.

Keywords: Brazilian Amazon, Socio-environmental indicators, Forest, climate, Hydrology, Agriculture, socio-economic development

Contents

1. Introduction

Monitoring and understanding socio-environmental dynamics in the Brazilian Amazon is a challenging task due to the large spectrum of socio-environmental concerns threatening this large territory. In order to monitor such dynamics, interdisciplinary approaches coupling environmental monitoring (mainly based on in-situ or remote sensing data) and socio-economic information are required. In this regard, the WP3 team of the ODYSSEA project experimented a set of indicators that we implemented for a few selected sites in the Amazon.

These indicators are presented in this document, which is separated in two main sections. The section 1 focuses on purely environmental indicators, referring to forest characteristics and dynamics, agricultural dynamics, climate change and hydrological resources. Section 2 introduces examples of socio-environmental indicators, built by crossing environmental indicators with social variables. It contains indicators about relationships between deforestation and socio-economic development, agricultural practices and climate, perception of climate change by local communities and health-environment studies.

2. Environmental indicators

2.1. Indicators of forest dynamics

2.1.1. Indicators of forest characteristics

Due to the natural diversity of forest types and variety (nature, intensity and frequency) of anthropogenic disturbances, multiple forest structures can be observed within forest landscape mosaics. Forest degradation determines gradients of alteration to forest structure and nowadays accounts for 68.9% of overall forest carbon losses. This calls for indicators characterizing the state of the forest as well as techniques to reliably assess those indicators from cost-efficient monitoring schemes.

Tropical rainforests display complex patterns of variation in reaction to factors that express themselves at different scales. A hierarchical approach is therefore needed. Remotely-sensed data that are the most informative, notably due to very high spatial resolution (VHSR) are generally restricted to limited surfaces owing to cost of purchase (for airborne or VHSR satellite images) or to time constraints of acquisition for field and unmanned aerial vehicle (UAV) airborne data. There is thus a need to define and use indicators

of forest structure that could be upscaled from best-documented reference sites to wider territories.

The aspect of forest canopy provides important indirect indicators of forest 3D structure, which itself reflects dynamical stages. Those indicators should be defined as to allow monitoring from remote sensing data of sufficient resolution or relevance. Vertical altimetry allows defining straightforward indicators pertaining to forest canopy maximal height (upper envelope of the crowns) or canopy height variation in space (canopy roughness). Associated metrics are generally relevant to predict forest biomass or to infer dynamical stages, though this inference is often context-dependent. Up to now, canopy altimetry was dependent upon airborne coverages using Lidar or radar sensors or to stereometry from VHRS satellite images. All those systems are costly and dependent on flight authorization. Canopy altimetry from UAV (see below) opens new prospects about cheap and agile acquisition though it will not allow covering large areas. Overall, reference airborne data should be put at the basis of upscaling chains that use space-borne data of decreasing resolution yet increased swath and affordability as to reach broad scale, wall to wall mapping of forest state indicators of known accuracy.

Upscaling from airborne reference altimetric data to satellite imagery could be based on another class of indicators pertaining to the notion of canopy grain. Grain (or texture) allows characterizing canopy optical images as soon as the contrast between sunlit and shadowed tree crowns becomes perceptible. This property increases with the fineness of image spatial resolution (Fig. 1). This explains why, in VHSR images (say, pixels of less than 2 m), the tropical forest no longer appears as a continuous homogenous photosynthetic layer, as it is the case on high to medium resolution images with greater pixel sizes (Fig. 1). Intuitively, the canopy grain depends on both the spatial distribution of trees within a scene, the shapes and dimensions of their crowns along with the characteristics of the inter-crown gaps. In fact, foresters and ecologists have long known that canopy aspect in 2D views provides useful information on forest structure, and visual interpretation of aerial photographs has been used in forestry since the 1950s, but few attempts were made to translate it into processing schemes of digital canopy images. Texture analysis of canopy satellite images can therefore be an objective, semiautomatic substitute to visual interpretation of the aerial photographs. It can also be applied to historical series containing digitized aerial photographs and satellite images.

Figure 1: Differences of canopy grain perception between two 300 m^2 subset images of different spatial resolution over a mixed savanna forest-inhabited area, French Guiana. Left: SPOT5 Fusion satellite image acquired in October 2010 (nominal resolution of 2.5-m, larger pixels actually). Right: a 20-cm pixels aerial photograph acquired in July 2010 (L'Avion Jaune). Drone now allows the acquisition of images having similar characteristics.

Methods

Sites selection

We tested the methods on two regions experiencing very contrasted patterns of human impact, i.e. a forested landscape with very limited human presence (Central Amapa) and a human-dominated landscape of Paragominas municipality (Para state, Brazil). The work in Central Amapa was carried out in synergy with the Biomap project (Guyamazon III funding framework) about "Integrating multiscale spatialized data for mapping forest types and biomass in Amapa and French Guiana (http://www.guyamazon.org/guyamazon-iii-2015-2018/biomap).

Texture analysis and FOTO method

Texture analysis of panchromatic canopy images allows the definition and monitoring of grain-based indicators by computing texture features from the spatial variation of gray-levels. The latter convey different meanings depending on the ecological context and the overall contrasts of vegetation.

For semiarid as well as for degraded vegetation, bright pixels usually correspond to bare soil, intermediate gray-scale levels to grass or vines cover, and darker pixels to woody vegetation. As a first approximation, gray-scale levels can thus be considered as a monotonically decreasing function of tree cover/biomass. On the contrary, in forest canopy images the interpretation is different since the fully sunlit crowns of canopy trees appear in white/light gray, while the shadowed inter-crown gaps are dark-grey or black. A monotonic relationship between gray-level scale and canopy height can thus be assumed in the absence of substantial relief-induced shadowing. In both cases, signal variation among neighboring pixels, i.e., texture, is relevant for providing indirect information on vegetation. Applications of texture analysis to forest canopy images can be based on several methods, among which Haralicks indices [1], lacunarity curves [2] or Fourier-based Textural Ordination (FOTO; [3, 4]. We will hereafter focus on the FOTO method.

Implementing the FOTO method (Fig. 2) means first subdividing images into windows of a size consistent with the targeted vegetation properties. To analyse forest canopies, a square window of about 1 ha is generally relevant and is consistent with a popular field plot size. Moreover, empirical trials have shown that the main textural gradients obtained, are to a large extent robust against variation in window size [5]. When applying FOTO, each of the windows originating from one or several digital images is submitted to a two-dimensional Fourier transform as to then compute the two-dimensional periodogram. Radial- or r-spectra are extracted from the periodogram as to furnish a simplified textural characterization (in terms of coarseness) This means summing the periodogram values (or entries) within ring-shaped concentric bins of unit width (same wave number) and neglecting information related to orientation and possible anisotropy. Spectra computed from many image windows of the same size are systematically compared using principal component analysis (PCA), which provides an ordination along a limited number of coarseness vs. fineness gradients. In so doing, windows are treated as statistical observations that are characterized and compared on the basis of their spectral profile, i.e., the way in which window gray-scale variance is broken down in relation to Fourier harmonic spatial frequencies. For all applications presented as illustrations, we applied the FOTO method in line with the procedure presented in Couteron et al. [6], Proisy et al. [4] and using routines developed in the MatLab environment (https://zenodo.org/record/1216005).

Data used for applications

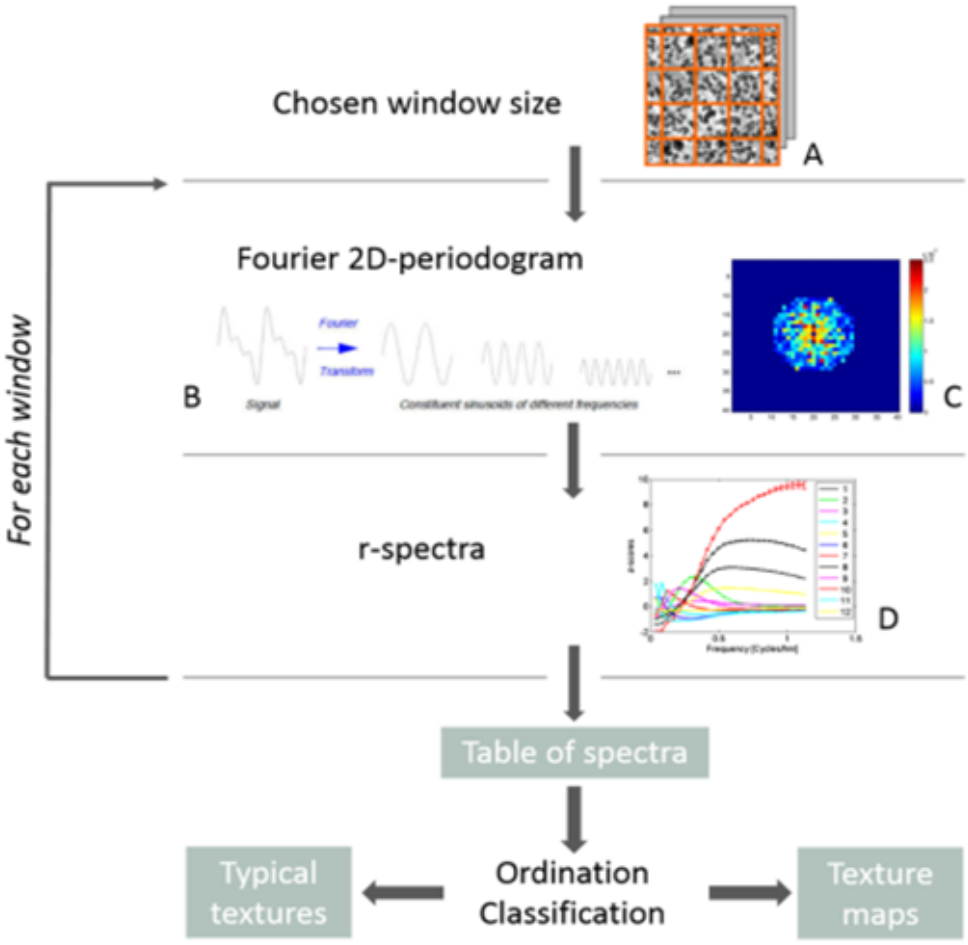

Figure 2: The steps of textural analysis with FOTO. (A) Process starts with subdivision of the analyzed image into square windows; (B) decomposition of signal at window scale by 2D Fourier transform; (C) 2D Fourier periodogram; (D) examples of r-spectra giving the proportion of variance explained by harmonic spatial frequencies for some hypothetical classes of texture. Fom Bugnicourt et al. [7].

Satellite canopy images

Very high spatial resolution (VHSR) imagery of approximately 1 m resolution, provided by satellites such as GeoEye, Ikonos, Orbview, Quickbird, or Pleiades, has now become widely available at an affordable cost or even

free over certain territories via Google Earth or different archives such as for Orbview. In the following, we show from recent studies that the increased availability of optical images of high to very high spatial resolution opens up new avenues for directly monitoring important vegetation properties such as above ground biomass and vegetation cover. These images can also provide indirect evidence of ecological processes that are shaping vegetation dynamics. Increased spatial resolution enables a move away from pixel-wise classification to schemes based on the analysis of textural properties of images at scales that are meaningful with respect to the vegetation properties under study. In the specific case of forest territories, VHSR greatly increases the potential for texture analysis of canopy images by enabling texture information to directly reflect the contrast between sunlit and shadowed tree crowns, and thus provide information on the size distribution of crowns and inter-crown gaps [6, 8, 9].

UAV images

Structure from Motion processing of UAV images offers a unique opportunity to identify and characterize these structures through digital canopy height models. Canopy texture metrics derived from VHRS images can quantify the coarseness gradient of canopy crowns and are relevant proxies for the assessment of tropical aboveground biomass. However, canopy texture metrics have rarely been used to study the large range of degraded forest structures. The aim of this study is: i) to characterize the structure of a wide range of degraded forests types using optical UAV imagery; to ii) investigate the relationship between canopy texture indices and a set of landscape and crowns metrics derived from canopy height model

Applications Illustrations in Amazonia

Canopy texture analysis from VHRS satellite images in Central Amapa

This case study was carried out as Mestrado application project of K.P. Cambraia dos Santos. The image used for applying the FOTO method was a SPOT 6 Satellite, acquired on October 22, 2015 for the BIOMAP project. The band used was the panchromatic mode (450-745 nm), with spatial resolution of 1.5 m, orthorectified with basic radiometric corrections.

FOTO was applied to this image thanks to a dedicated program (freely downloadable from https://zenodo.org/record/1216005),using an image window size of 180 m and a distance between centers of overlapping windows

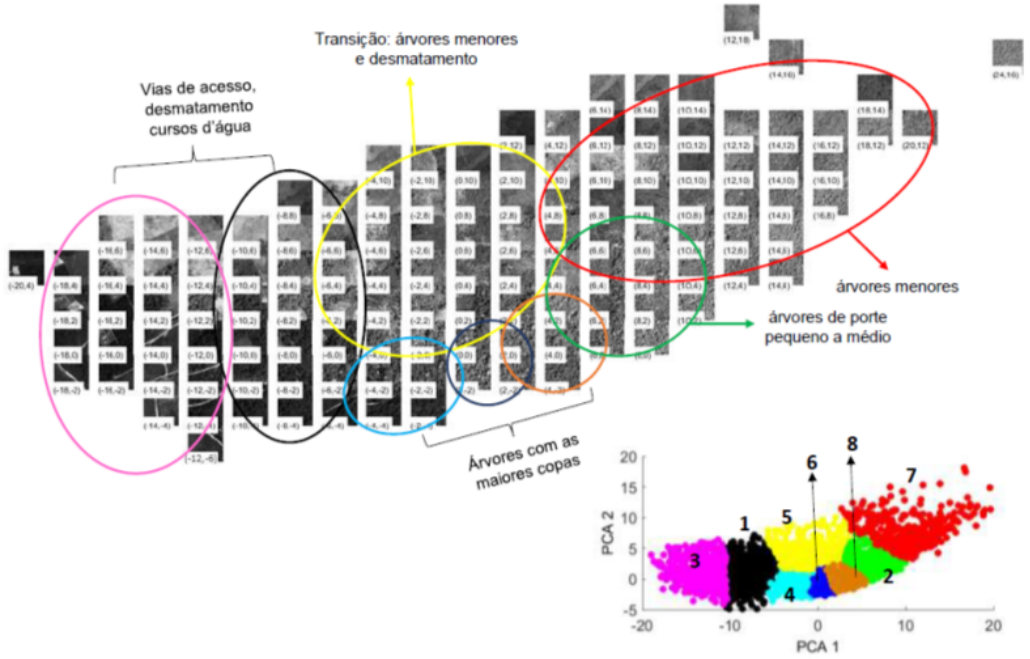

Figure 3: Results provided by the FOTO method applied on a SPOT6 VHSR image over Central Amapa. The texture gradients highlighted by the PCA on Fourier r-spectra (plane PCA1 vs. PCA2) are illustrated by typical windows. Classes yielded by the k-means clustering (insert bottom-right) are indicated as circles around the displayed windows with the same color chart.

of 54 m. Scores along the first three PCA axes were used as texture indices to order windows along texture gradients that explain the maximal share of variance between r-spectra values. These three PCA axes can be mapped as a RGB image. The first PCA axis opposed coarse textures (large share of image variance accounted for by small spatial frequencies) to fine textures (large spatial frequencies) while the second axis put emphasis on intermediate frequencies (Fig. 3). K-means clustering was also applied to r-spectra as to provide textural classes that were mapped on Fig.3. After several preliminary tests, eight texture classes were retained and mapped.

The classes that best represent the canopy grain gradient are along the lower fringe of the windows cloud in the PCA plane (Fig. 3). The lower left corner (coarsest textures induced by a macro-heterogeneous structure) features road, rivers and trails (classes magenta and black). On Fig. 4 (right),

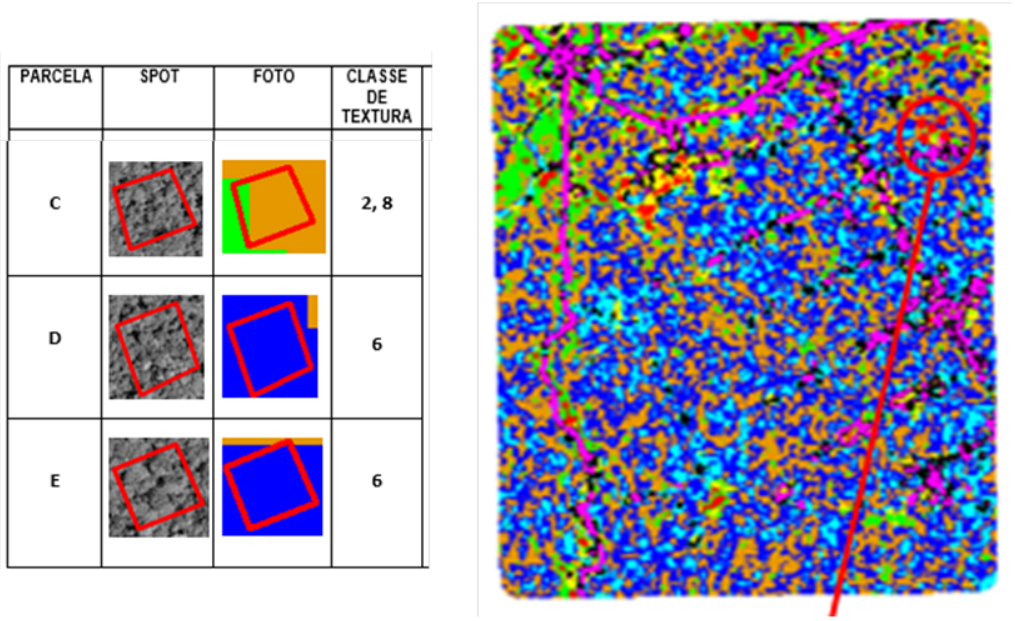

Figure 4: Interpretation of the textural mapping from the comparison between canopy aspect for some field and texture classes (on the left) and the overall mapping of texture classes (on the right).

road and trails are clearly apparent thanks to the magenta class.

The classes that best represent the canopy grain gradient sensu stricto are coarse-intermediate textures associated to large crowns (cyan and blue) to fine textures, referring to small crowns and regeneration in altered forests(green and red). Field plots allowed illustrating the meaning of texture classes in terms of canopy aspect (Fig. 4, left). The texture class map on the right side of this figure exemplify how texture analysis can help grasp the main features of a forested landscape with limited scars of human penetration. The linear shapes associated to the magenta class allows locating roads and trails, while the black class mainly points toward crops. Classes of fine-grained forest canopy (red, green, yellow) are mostly fringing those two classes and can be interpreted as capoeiras or highly degraded forests. The canopy texture gradient in areas distant from anthropogenic disturbances mostly reflected the transition from medium-sized to large crowns (classes cyan, blue and brown-orange),which altogether cover most of the area.

Using canopy metrics from UAV to assess the structures of Amazonian

degraded forests

Twenty-two UAV images of 25 ha each (10 cm resolution) were acquired in September 2017 along the whole forest degradation gradient observable in Paragominas, Para. Forest status were evaluated from field observations based on the forest structure, the visible impacts (fire and logging) and the information on forest stands. From these images, we derived three sets of canopy metrics (Fig. 5):

- Canopy height metrics: the Digital Surface Models were derived from Motion and MultiView Stereo processing (Pix4d software);
- Textural metrics: we derived the Fourier Transform Textural Ordination - FOTO spectrum and the lacunarity index based on the spatial variation in pixel radiance,
- Crowns metrics: object based segmentation of DSM allowed to identify three vegetation stratum (bare soil, regeneration-low ligneous, and dominant-emergent trees of the canopy). We delineate major canopy crowns and computed crowns width, area and length.

We first analysed the relationships between canopy altimetric variables (median height, standard deviation, etc) and forest status (Fig. 5). Highly degraded forests due to illegal logging and recurrent understory fire events are characterized by low and heterogeneous canopy structures (low median height, high coefficient of variation) whereas conserved and RIL (Reduced Impact Logging) forests have high, closed and homogeneous canopy structures.

FOTO captures the gradient of canopy crown coarseness-fineness especially by opposing low spatial frequencies (v5 to v9) and high spatial frequencies (> v14) which tend to be strongly inter-correlated (Fig. 6, PCA1), and by sorting out intermediate frequencies (around v10-v11). Canopy textures of slightly degraded forests are dominated by large crowns (A, see figures 6 and 7) while highly degraded forests appeared dominated by small crowns (D and E).

Generalized Linear Models were established as to explain the canopy heights and roughness metrics (standard deviation, coefficient of variation, etc) from the FOTO and lacunarity texture features. The combination of FOTO and lacunarity textural metrics leads to a significant relationship with the standard deviation of canopy height (R=0.54).

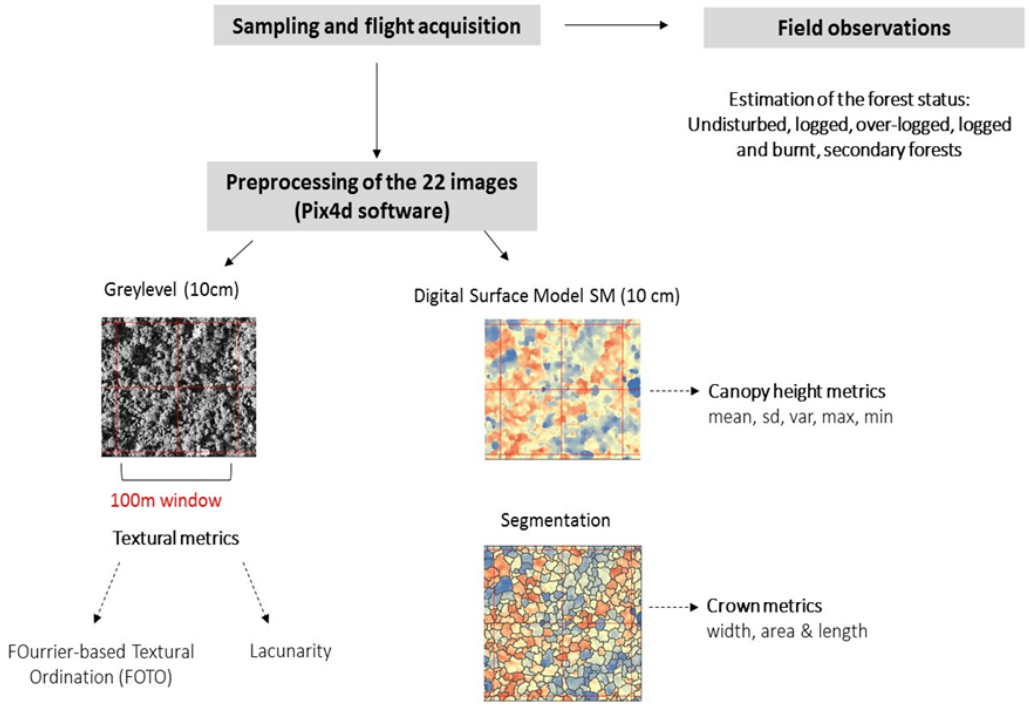

Figure 5: Data collection and analysis processes.

The increased availability of UAV images raises the opportunity to compute digital canopy elevation within the forest landscape and thus train models using VHSR optical images to assess the structure and status of degraded forests.

Conclusion

To conclude, we have here introduced and exemplified that canopy texture (in a general sense) can be consistently quantified as to provide texture indices that have strong interpretative power in terms of stand structure or in terms of openings of the forest canopy. In other words, texture features easily translate into indicators of forest degradation. At landscape scale, the relative distribution of texture classes also informs on the levels and modalities of human activities, and may be the source of further pattern analysis as to assess indicators of transformation of forest landscapes (e.g. fragmentation, frequency of roads, etc). With this respect, the FOTO method ordinates canopy image windows along texture gradients that generally agree with vi-

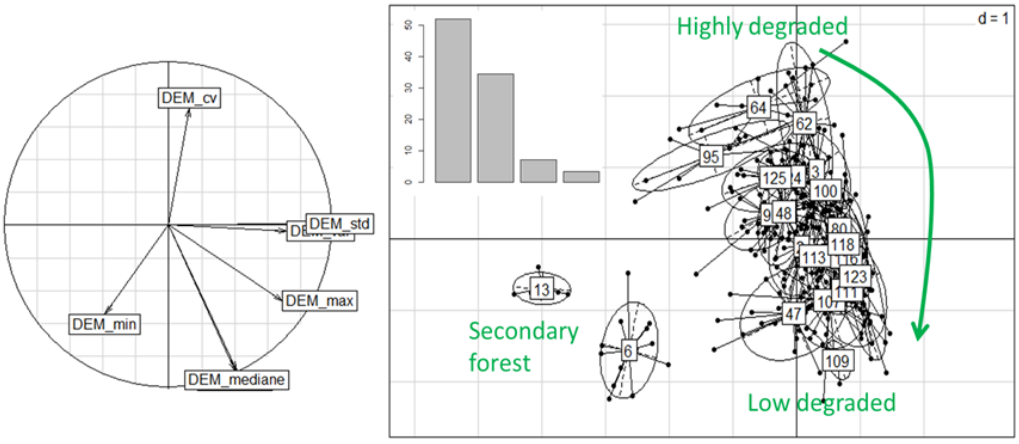

Figure 6: Canopy height structures obtained after Structure from Motion and MultiView Stereo techniques for the plots covered by the 22 UAV flights. ACP correlation circle for DEM/DSM variables (left) and plots locations in the first PCA plane with results of s-class clustering (right).

sual interpretation [6, 10], see also figure). FOTO textural indices enabled the retrieval of stand structure variables, among which above-ground biomass (AGB) gradients in several case studies across the tropics [4, 11, 12, 13, 14], with costs 50 to 100 times lower than airborne Lidar. The FOTO method also appeared promising for detecting diachronic changes in the canopy, such as tree fall gaps, skid trails or crown enlargement [15]. However, there also are situations for which texture features, including FOTO and other families of features (e.g. lacunarity; [2]), failed to capture forest structure gradients with sufficient accuracy [16].

The interpretation between stand structure and canopy texture is in fact context-dependent. And the way in which texture features relate to stand variables strongly varies across forest types [17]. This is particularly true when using satellite images having pixels approaching the maximum size that allows detecting crown size signature (say, about 2 m). Deriving indicators from canopy texture features on a safe basis impose to learn from reference data which types of vegetation cover are actually behind a given class or a certain gradient of texture. The most natural reference data are field plots or transects, but it is generally impossible to get enough of them to have a sufficient sampling across a very wide area displaying a variety of causes

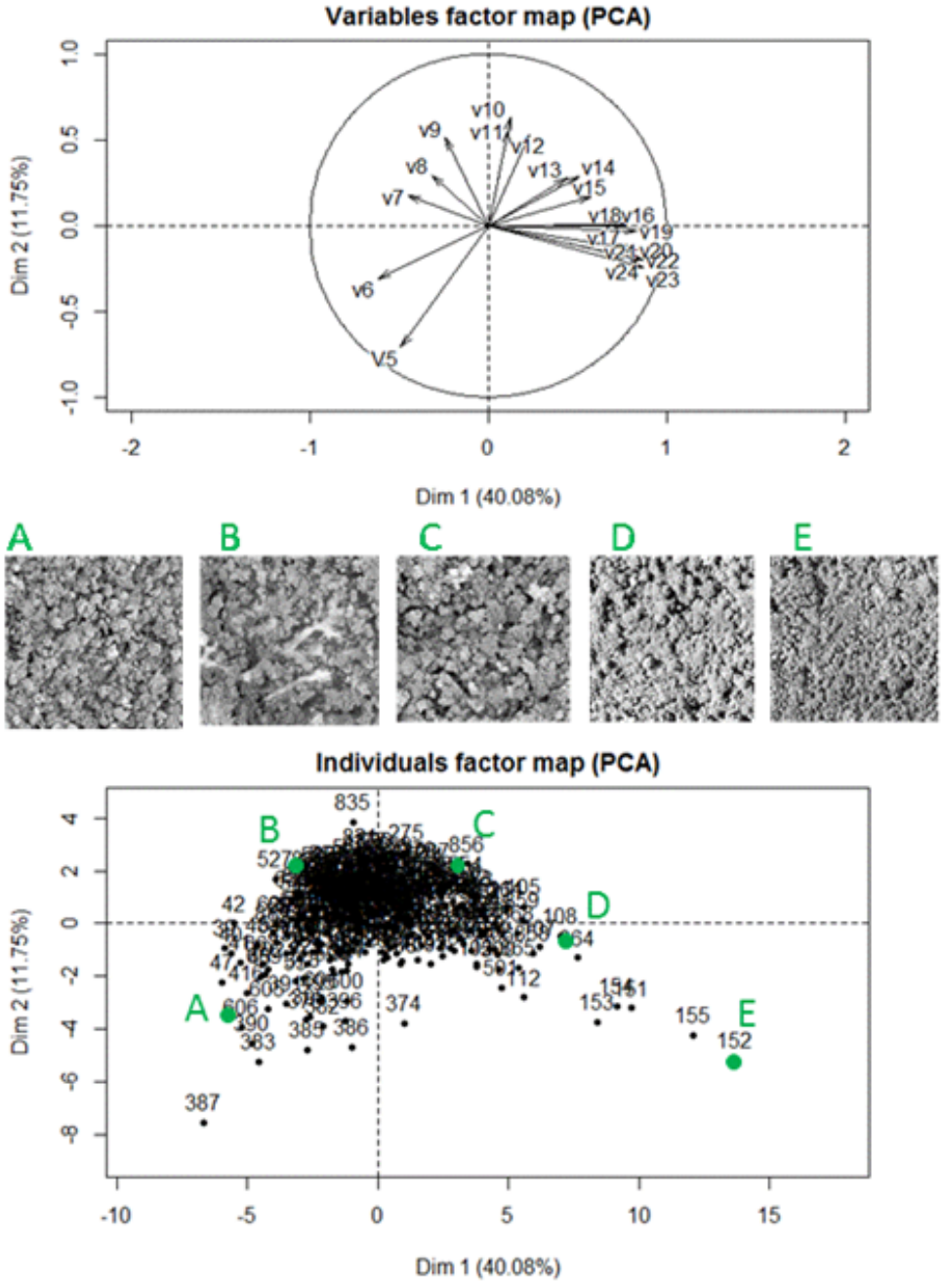

Figure 7: Canopy texture ordinations based on the FOTO method: correlation circles with variables numbered as increasing spatial frequencies (top); scatter plot of PCA scores along the first two principal axes along for imaged plots. Five samples are shown (from A to E) for illustrating the degradation gradient (middle).

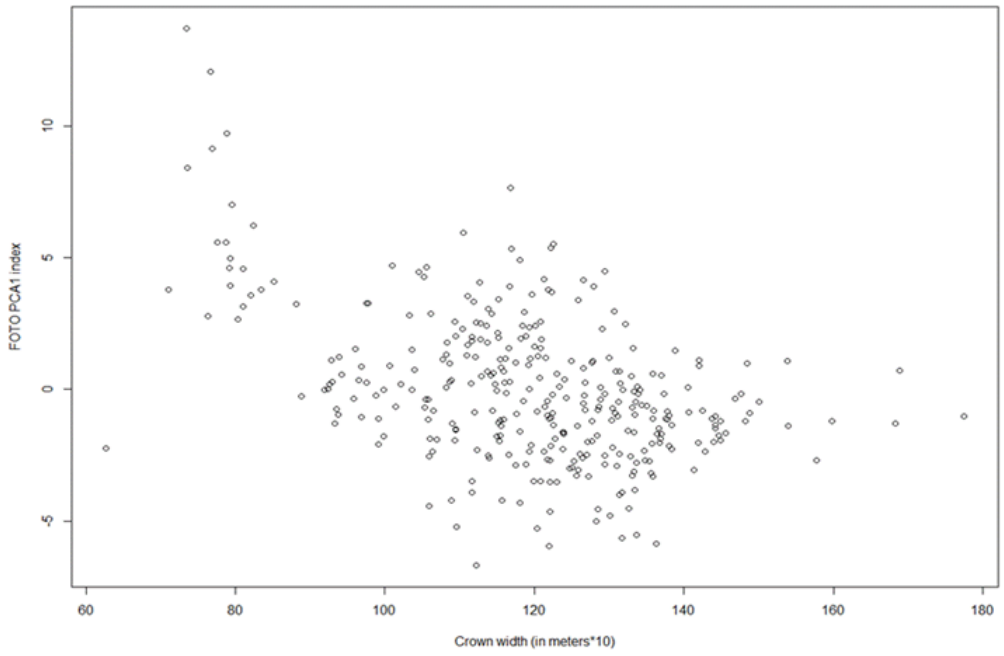

Figure 8: Relationships between crown width (from delineation on the DSM) and the first axis of the FOTO PCA.

of forest structure variation. UAV now provide appealing perspectives for getting reference data of very high interpretability, and for increasing the cost-efficiency of ground-truthing.

UAV images can provide altimetry metrics of the forest canopy at a far lower cost than plane-borne Lidar of photogrammetric solutions (though the quality of the UAV-based canopy altimetry may be questioned in rough terrain). The present application illustrates how one may in the future perform context-specific calibration of texture features from drone-based altimetry metrics. These latter are known to generally correlate with stand structure variables [18, 19] that are currently measured in the field. On the other hand, texture features from VHSR satellite images of sufficient resolution (say pixels $<$ c. 2m) would be useful to grasp what free high to medium resolution imagery (i.e. pixels from 10 m to 250 m) can tell about gradients of forest structure, especially those relating to forest degradation. Overall, texture should not be seen as a substitute to classical reflectance-based approaches to vegetation cover of landscape structure, but rather as a source

of complementary information.

2.1.2. Indicators of fire dynamics

Large areas of savanna and woodlands in tropical regions burn every year. Occurring mainly during the dry season when herbaceous vegetation has dried out, fires are one of the main drivers of ecosystem transformation or maintenance [20]. Land management practices induced by human activities are at the base of the majority of fire occurrences in the tropics. Shifting cultivation,agricultural expansion, deforestation and harvesting are some of the practices involving fires that may contribute to partial or complete destruction of vegetation cover, depending on fire intensity and combustion efficiency [20, 21]. Therefore, accurate and multi-temporal burned area maps are important tools that can help fire and land managers understand and assess the impacts of specific interventions, while informing landscape management strategies.

Multi-temporal data records of fire distribution, extent, and timing, correspond to historical activity data, which together with vegetation emission factors, support the quantification of emissions. The establishment of emission baselines against which the results of subsequent vegetation and fire management actions can be compared is essential for the Measuring, Reporting and Verification (MRV) activities necessary in carbon accounting procedures. Thus, accurately and frequently mapping burned areas over large extents, using cost advantageous, periodic, and expedite approaches is very desirable.

Even though classification of burned areas using Landsat images provide satisfactory results with classical approaches [22], the spectral similarities between burnt surfaces and other land cover categories, such as, water bodies, shadows, and mixed water-vegetation, still introduce spectral confusion and overlap with other classes. Therefore, it is important to explore new methods capable of increasing the discrimination between burns and other landscape features, minimizing the uncertainties [23, 24].

Genetic Programming (GP), one of the most powerful and underused methods of machine learning, was used for identifying and mapping burned areas in Landsat ETM+/OLI imagery. Its performance was compared with two classical methods: Maximum Likelihood classification (MLK) and Classification and Regression Tree analysis (CART). The research was conducted over three study areas located in tropical regions: Brazil, Guinea-Bissau, and the Democratic Republic of Congo (Figure 9). These areas are subject to

frequent and extensive fires, mainly due to human activity. The performance of each method was assessed by calculating the overall accuracy, Dice and Kappa coefficients, and omission and commission errors over a representative sample grid of points photo-interpreted according the classes burn/unburned. Also, the agreement of the classifications with surrogate ground-truth burned area maps (obtained from visual interpretation and on-screen digitizing of burned area perimeters over the entire images) is calculated based on precision and recall measures.

We compared three different methods (GP, CART and MLK) for detecting burned areas in three different sites (Brazil, Guinea-Bissau and Republic Democratic of Congo). The results showed that, depending on the study area and sensor type, the three methods achieved different accuracies. The accuracies of the burned area maps produced by the GP methods were always higher than those produced by CART, and only at the BRZ site GP performed worse than MLK, being affected by a small percentage of mislabeling errors (collected during the training step). GP methods at the DRC and GB sites present the highest values of overall accuracy and Dice and kappa coefficients. However, the commission and omissions errors varied considerably depending on the classifier and study site.

A detail of fire perimeter agreement between the ground-truth maps and the classified burned areas is shown for Area 1 of each of the three locations in Figure 10. Visual comparison between the classified maps and the satellite images shows distinct performance patterns according to the site location and classification method adopted. GP revealed to be a very versatile classification method, obtaining some of the best results. Despite the relatively high Dice and kappa (higher than 0.90 in some cases) and accuracy levels (higher than 99% in some cases) of the different classifiers, many fire scars were missed, and other areas were incorrectly mapped as fires (for example, shadows due to the topographic effect). Thus, further research is needed to establish the degree of improvement that can be achieved by the GP methods mainly in multi-temporal applications.

This work has been published in Silva et al. [25] and Cabral et al. [26]

2.2. Indicators of agricultural dynamics

Agricultural ecosystems provide and rely on provisions (i.e., food, fuel, timber), support (i.e., soil fertility), cultural services (i.e., recreation, spiritual services) and regulation (i.e., flood control, pollination, biodiversity).

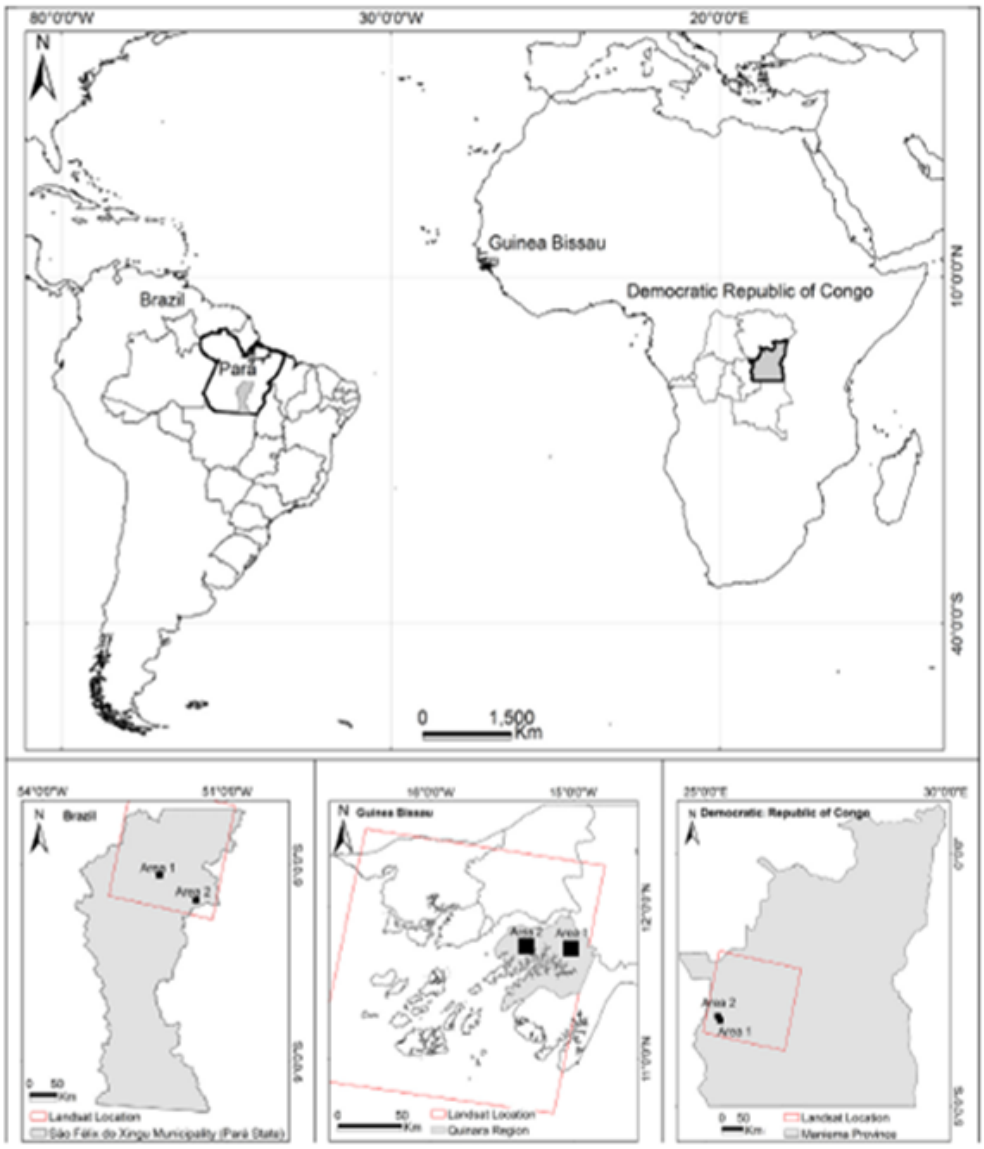

Figure 9: Study area.

Historically, farmers have focused on improving these ecosystems provisioning services by increasing the food production via agricultural expansion to address the needs of a growing population. Since the 1950s, the drastic growth of the world population has highlighted the limits of the agricultural

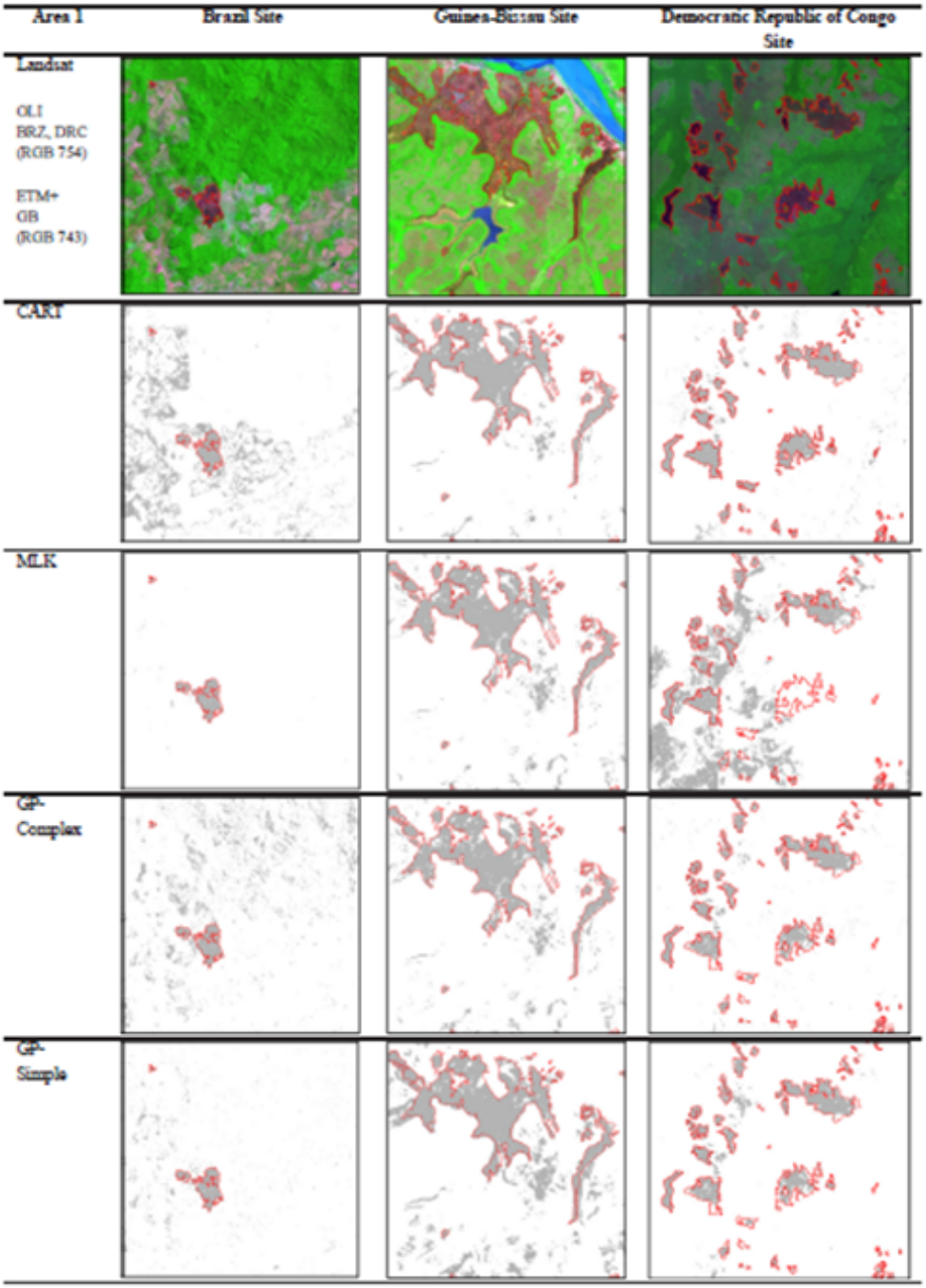

Figure 10: Landsat OLI (RGB 754) and Landsat ETM+ (RGB743) color composites crops corresponding to area 1, located at the small squares of Fig. 1, together with the burned area maps (in grey) derived from the three classification methods for each study site. The red line polygons delimit the ground-truth fire perimeters.

expansion models capacity to provide sufficient food. More intensive agricultural practices were then adopted during the Green Revolution [27, 28]. However, this new model has also been criticized because of its impacts on the ecosystems support, cultural and regulatory services. For these reasons, nowadays farmers are expected to adopt new practices to improve or maintain the ecosystems provisioning services while maintaining and/or retrieving the systems support, cultural and regulatory services. Such new model has been named ecological intensification [29]. The evolution from an agricultural expansion model toward an ecological intensification model can be described as a transition toward agricultural sustainability. All agricultural regions are expected to experience this transition.

In the Brazilian Amazon, the agricultural transition started much later than in temperate areas because the agricultural expansion model remained the main method for increasing the agricultural production for a long time. However, new agricultural practices are being rapidly disseminated as societies are becoming increasingly concerned with environmental issues. Here, we focused on the state of Mato Grosso (Southern Amazon) known as first national producer of important agricultural commodities such as soybeann. At the beginning of the colonization process, farmers used to plant soybean in single cropping systems. However, single cropping systems have been called into question because of their harmful environmental and economic impacts. To reduce their environmental and economic vulnerability, the soybean producers changed their agricultural management practices. In the 1990s, they started planting a second non-commercial crop (i.e., generally millet or sorghum) after the soybean harvest such that the residual vegetation from the second harvest allowed the producers to adopt a no-tillage practice. This practice is especially useful for improving the soils quality by limiting the loss of chemical products and organic matter via erosion and by retaining water for a longer period, which allows farmers to achieve better yields. In the early 2000s, the farmers began cultivating other commodities such as corn and cotton in double cropping systems, thus after the soybean harvest. In this way, new management practices improved the diversification process, optimized the use of fertilizers and helped fight against crop diseases.

To monitor the evolution of Mato Grossos agricultural systems, we must obtain accurate agricultural statistics. We then designed a methodology to clarify the land use changes observed in Mato Grosso in terms of the agricultural transition process based on remote sensing data. Based on agricultural maps derived from the analysis of MODIS times series (MOD13Q1 product

Agricultural model	Index code	Index definition	Unit
Agricultural expansion	NC	Annual net cropped area	km^2
	DEF	Proportion of deforestation that occurred from 2001 to 2004 because the forest land was directly converted into croplands	%
	EXP	Proportion of agricultural expansion from 2002 to 2003 and from 2005 to 2006 because of direct conversions of native vegetation into croplands	%
Agricultural intensification	DC	Annual area cultivated with double cropping systems utilizing two commercial crops from the cropping years in 2000–2007	km^2
	DC/NC	Annual proportion of the net cropped area cultivated with double cropping systems involving two commercial crops	%
	DC/TC	Annual proportion of the total cropped area cultivated with double cropping systems involving two commercial crops	%
Ecological intensification	PC/NC	Annual proportion of the net cropped area permanently covered by vegetation during the rainy season	%
	ADI	Annual measure of the Area Diversity Index (Eq. (1))	Unitless

Figure 11: List of indicators used to characterize the agricultural transition from the cropping years in 2000-2007.

; [30]), we defined a set of indicators on the three stages of the agricultural transition process: agricultural expansion, agricultural intensification and ecological intensification (Fig. 11).

2.2.1. Indicators of agricultural expansion

Agricultural expansion consists of converting land into cropland and is described by the evolution of the three indices. We calculate the annual NC (Net Cropped) index by using the agricultural maps derived from the MODIS Terra/EVI time series. NC refers to the Net Cropped area (i.e., the agricultural area) independently from the cropping system applied to the area. We use the index to quantify the evolution of the Net Cropped area from 2000 to 2006 for each ecoregion (i.e., forest and cerrado) in the entire state of Mato Grosso. The next two indices, DEF and EXP, describe the

direct expansion of agricultural land in relation to the deforestation process. Direct agricultural expansion refers to the process of converting previously unused areas of natural vegetation into new production areas. First, the DEF index represents the proportion of deforested land in which a crop has been detected at least once during the two years following the clearing of the land. Second, the EXP index represents the proportion of agricultural expansion that was observed in recently cleared areas (i.e., up to two years before the first crop was detected).

In Mato Grosso, the net cropped area (NC) expanded by 43% between 2000 and 2007 (Fig. 12). Although the net cropped areas of both ecoregions rapidly increased at the state level, the areas expanded at different rates for each ecosystem. The rate of agricultural expansion was more pronounced in the forest ecoregion than in the cerrado ecoregion. The major agricultural expansion occurred in the Central and Eastern agricultural regions (i.e., regions B and D, respectively, in Fig. 13), both of which are mainly located in the Amazonian forest. The DEF index indicates that 12.6% of the deforested area in Mato Grosso was directly converted into cropland from 2001 to 2004 (i.e., within two years after deforestation). This result implies that other important drivers of deforestation, such as cattle ranching or timber, may have had a more important impact on deforestation in Mato Grosso than crop expansion. However, the DEF index calculated at the Mato Grosso scale corresponds to an area of 7771 km2, of which 4950 km2 consisted of forest land. Thus, the direct impact of mechanized agriculture on deforestation cannot be understated. In addition, the EXP index indicates that 27% of the crop expansion that occurred during the cropping years from 2002-2003 to 2005-2006 was based on direct conversions of native vegetation areas into cropland. Although this rate may also appear to be low, it represents 4796 km2 at the state level. Both indices indicate that the direct link between agricultural expansion and deforestation is stronger in the forest ecoregion (DEF = 15.7%; EXP = 33%) than in the cerrado ecoregion (DEF = 8.7%; EXP = 19%).

2.2.2. Indicators of agricultural intensification

Agricultural intensification occurs if an area experiences higher levels of both inputs and outputs (in quantity or value) of cultivated or reared products per unit area and time (Lambin et al., 2001). Thus, we assumed that double cropping systems involving commercial crops (i.e., soybean, corn and cotton) constitute a type of agricultural intensification because these systems

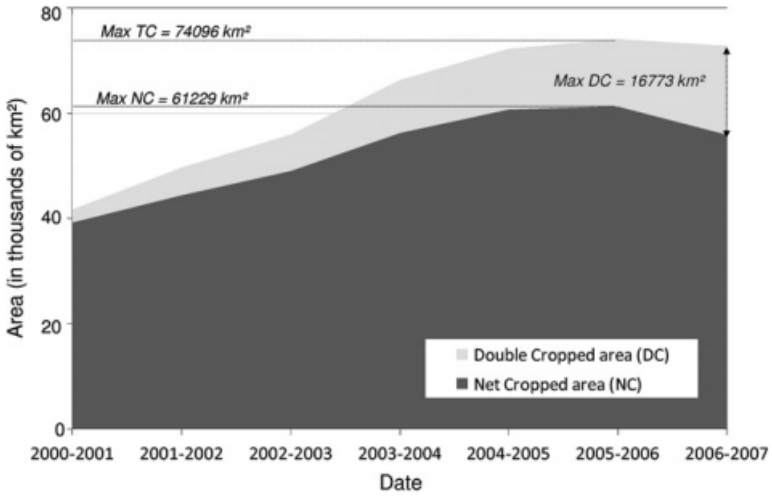

Figure 12: Annual evolution of the Net Cropped (NC) and the Double Cropped (DC) areas in Mato Grosso from the cropping years in 2000-2007. Total Cropped area (TC) corresponds to NC+DC.

increase both inputs and outputs in one area. We did not consider double cropping systems involving non-commercial crops (i.e., millet or sorghum after a soybean harvest) because farmers adopt these systems not to increase their outputs but to protect the soil from erosion, improve the soils quality, break the pest cycles,maintain the soilsmoisture and set the conditions for high-quality no-tillage operations (Landers, 2001). Following this assertion, we calculated three indices based on the agricultural maps issued from the MODIS EVI time series to identify the importance of the agricultural intensification process (Table 1). We used the DC (Double Cropping) index to quantify the evolution of the double cropping area for each ecoregion (i.e., forest and cerrado) in the entire state of Mato Grosso from 2000 to 2006. DC refers to the agricultural area cultivated with double cropping systems involving two commercial crops (i.e., soybean, corn or cotton). We calculated the DC/NC (Double Cropping area/Net Cropped area) index to measure the evolution of the annual proportion of the net cropped area sown with double cropping systems involving two commercial crops. This index is an indicator of the arable lands intensification levels. We then used the DC/TC (Double Cropping area/Total Cropped area) index to estimate the evolution of the proportion of the total cropped area sown with double cropping

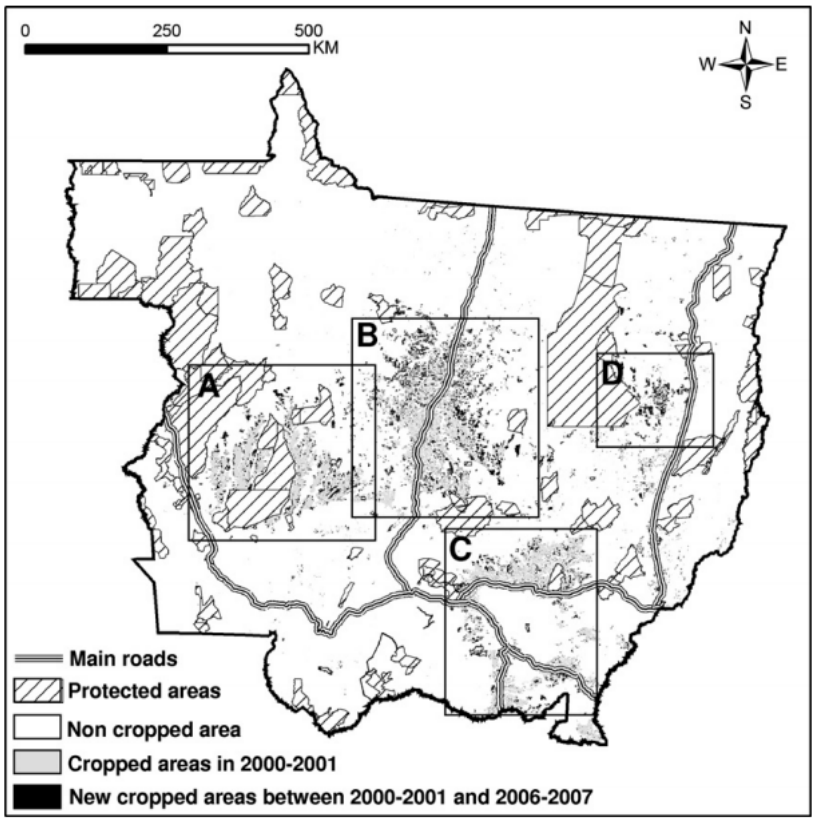

Figure 13: Agricultural expansion in Mato Grosso. The four main agricultural regions are the following: (A) the Parecis plateau, (B) the BR163 region, (C) the Southeastern region and (D) the Eastern region.

systems involving two commercial crops. TC refers to the Total Cropped area calculated by adding NC and DC. Unlike the Net Cropped area, this index is linearly linked to the agricultural production. This DC/TC index is then an indicator of the proportion of the agricultural production caused by agricultural intensification.

The area cultivated with double cropping systems involving two commercial crops (DC index) increased constantly and drastically (590%) from 2442 km2 during the 2000-2001 cropping year to 16,773 km during the 2006-2007 cropping year (Fig. 14). As a result, the proportion of the net cropped area sown with two successive commercial crops (DC/NC index) increased from 6% in 2000-2001 to 30% in 2006-2007 (Fig. 14). We found the same

conclusion when we observed the annual proportion of the total cropped area cultivated with double cropping systems utilizing two commercial crops (DC/TC index) (Fig. 14). This area increased from 5.8% to 23%, which indicated that nearly one quarter of Mato Grossos agricultural production was based on intensive agriculture. Both indices showed similar increasing patterns, with a common spike in intensive agriculture during the 2006-2007 cropping year. This spike is explained by the decrease in NC combined with an increase in DC during this year. Our results indicated that from 2000 to 2006, the total cropped area in Mato Grosso increased faster than the net cropped area because the farmers implemented many double cropping systems with two commercial crops. We estimated that during these seven cropping years, 46% of the increase in the total cropped area was due to the adoption of intensive agricultural management practices. The maps of agricultural intensification (Fig. 15) indicate that agricultural intensification experiences a strong level of spatial variability at the regional level. For all of the agricultural intensification indices (DC, DC/NC and DC/TC), the results were higher in the cerrado ecoregion than in the forest ecoregion.

2.2.3. Indicators of ecological intensification

The principles of ecological intensification are based on the adoption of new agricultural management practices designed to improve fertilizer efficiency, improve water use efficiency, maintain and retrieve soil fertility, and improve the monitoring of crop diseases. We defined two indices to analyze the ecological intensification process. First, the PC index (i.e., the area permanently covered by crop vegetation during the rainy season) represents the proportion of the net cropped area that is permanently covered by a crop during the entire rainy season for each cropping year. We considered the areas cultivated with double cropping systems that involve both commercial (i.e., corn, soybean, cotton) and noncommercial crops (i.e., millet and sorghum) to be permanently covered by crops. We consider this index to be a sign of ecological intensification because it allows farmers to improve soil quality, break pest cycles, maintain soil moisture, and set the conditions for high-quality no-tillage operations for the following soybean crop. In addition, the Area Diversity Index (ADI) proposed by Ray et al. [31] allowed us to measure the level of crop diversification based on equation 1:

$$ADI = \frac{1}{\sum_{i=1}^{n}(a_i/\sum_{i=1}^{n} a_i)^2} \quad (1)$$

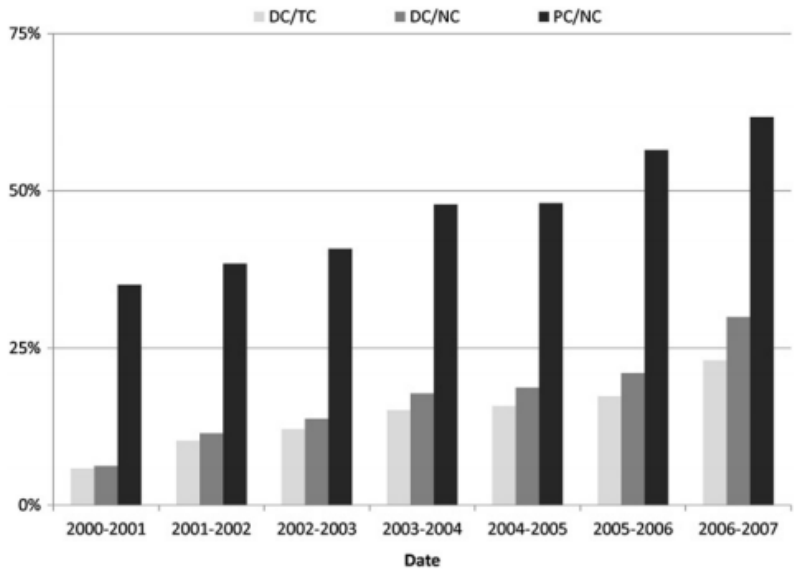

Figure 14: Annual evolution of the proportion of the total cropped area cultivated with double cropping systems using two commercial crops (DC/TC), the proportion of the net cropped area cultivated with double cropping systems using two commercial crops (DC/NC), and the proportion of the net cropped area permanently covered by vegetation (PC/NC) indices in Mato Grosso from the cropping years in 2000-2007.

where a_i is the area sown with the *ith* crop. The maximal value of ADI is the number of crops that are considered. Here, we considered four crops : soybean, corn, cotton and the non-commercial crops. Thus, in this study, ADI = 4 indicates that cultivated areas for soybean, corn, cotton and non-commercial crops are equal. In contrast, ADI = 1 indicates that a monoculture situation exists.

In Mato Grosso, the proportion of the net cropped areas permanently covered by vegetation (PC/NC) increased drastically from 35% in 2000-2001 (13,741 km2) to 62% in 2006-2007 (34,543 km2) during the study period (Fig. 12). This practice allowed the producers to not only improve the quality of the soil and the efficiency of their water use but also enabled them to adopt notillage practices during the following soybean harvest to improve their yields. For the producers, implementing double cropping systems with commercial and non-commercial crops represented the best method for diversifying agricultural production. The evolution of the Area Diversity Index, which increased from 2 to 2.51 during the study period, confirms this notion

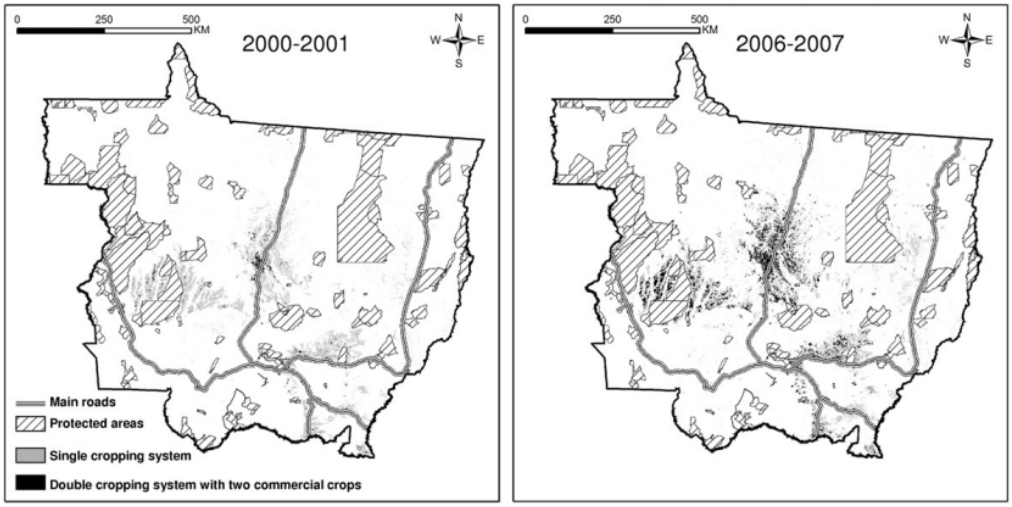

Figure 15: Agricultural intensification in the state of Mato Grosso in 2000-2001 and 2006-2007 cropping years.

(Fig. 16). This evolution is mainly explained by the large increases in the areas sown with corn, cotton and non-commercial crops. Fig. 16 also indicates that the ADI is much higher in the cerrado ecoregion than in the forest ecoregion.

2.3. Indicators of hydrological dynamics

2.3.1. Indicators of anthropization of hydrological resources

The last decade testified of a very dynamic agricultural frontier in the Southern Amazon with a high potential for the rapid adoption of a new agricultural model engaged towards intensification and diversification. Yet, beyond its positive impacts on deforestation, intensifying and diversifying the production also implies new pressures on natural resources. For example, the generalization of intensive double-cropping systems requiring high amounts of agrochemicals Arvor et al. [32], the adoption of irrigation systems to prevent harvest losses for the second crop and the development of fish farming raise important concerns about the future of soil and water resources in the region [33]. In this regard, the proliferation of small artificial water reservoirs to ensure crop irrigation, water livestock and farm fishes calls for special attention.

Scientific knowledge about the impacts of water reservoirs is partial since

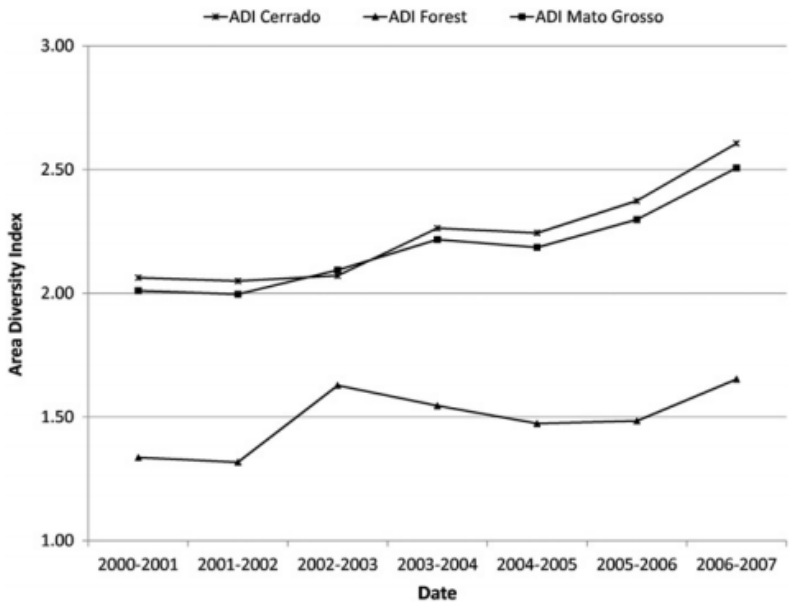

Figure 16: Evolution of the Area Diversity Index between the 2000-2001 and 2006-2007 cropping years.

most studies focus on major dams, especially in tropical regions such as the Amazon where the construction of numerous hydropower dams has drawn the attention of the scientific community [34, 35, 36]. Conversely, small reservoirs have received less attention despite several studies led in various regions of the world have shown that their multiplication can generate significant cumulated effects on chemical fluxes (e.g. Powers et al. [37]), fish communities (e.g. Santucci et al. [38]) and hydrological cycles (e.g. Habets et al. [39]). In this specific regard, various studies concluded that a high number of dams, although small when considered individually, can have similar or even greater impacts than one single large dam [40, 41, 42].

Whereas methods and models to assess the individual and cumulated impacts of dams exist [39], mapping and counting the small artificial reservoirs at regional scale still appears as a major bottleneck for this type of application [43]. This point is of extreme importance since the spatial distribution of the water bodies (i.e. density, position in the basin, etc.) is known to be crucial to assess their cumulated effects [44]. In this regard, we implemented a fully automatic procedure to classify water reservoirs based on time series

of Landsat images. Once the data were acquired, the method to process the images was made of five main processing steps: (1) data were pre-classified, (2) two indices were computed for each scene-year based on the analysis of time series, (3) the indices were mosaicked on the entire area, (4) annual water masks were produced and (5) inter-annual transition rules were applied. Finally, the method includes a validation step (6) to assess the accuracy of the produced maps. Based on these maps, we derived two indicators of the anthropic pressure on hydrological resources : (1) the number of water reservoirs and (2) the cumulated area of water reservoirs. Further indicators are currently being implemented in order to better take into consideration the position of reservoirs in the basin (e.g. distance from source, etc).

We mapped all water bodies in the municipality of Sorriso (state of Mato Grosso), known as the first producer of soybean in Brazil (fig. 17). We then monitored the rapid expansion of water bodies during the last thirty years (Fig. 18). The cumulated area increased from 153 hectares (mean value between the low and high estimates) in 1985 to 1707 hectares in 2015, i.e. the area of a medium-size farm in the region (Fig. 18, top). The cumulated area thus increased more than tenfold in thirty years. The results showed an especially rapid proliferation after 2000 corresponding to the period of agricultural intensification in the region (Arvor et al., 2012), which was partially based on irrigation thus requiring increased access to water resources. The number of water bodies also increased rapidly during the study period, from 86 to 522 (mean values of 1985 and 2015) (Fig. 18, bottom). In addition, the number of water bodies increased rapidly (+50%, from 347 to 522, mean values) between 2010 and 2015 whereas the cumulated area only increased moderately (+14%, from 1494 to 1707 ha, mean values). It means that the numerous water bodies created during that period were quite small. This increase may reveal tendencies on the recent development of numerous small excavated dams dedicated to fish farming, which could not be accurately delineated at Landsat scale but whose detection may be used as a proxy to observe the process of agricultural diversification in the southern Amazon.

This work has been published in Arvor et al. [45]

2.4. Indicators of climate change

Climate change in the Amazon region is the subject of many studies not only due to its stance as an emblematic ecosystem but also as a region where

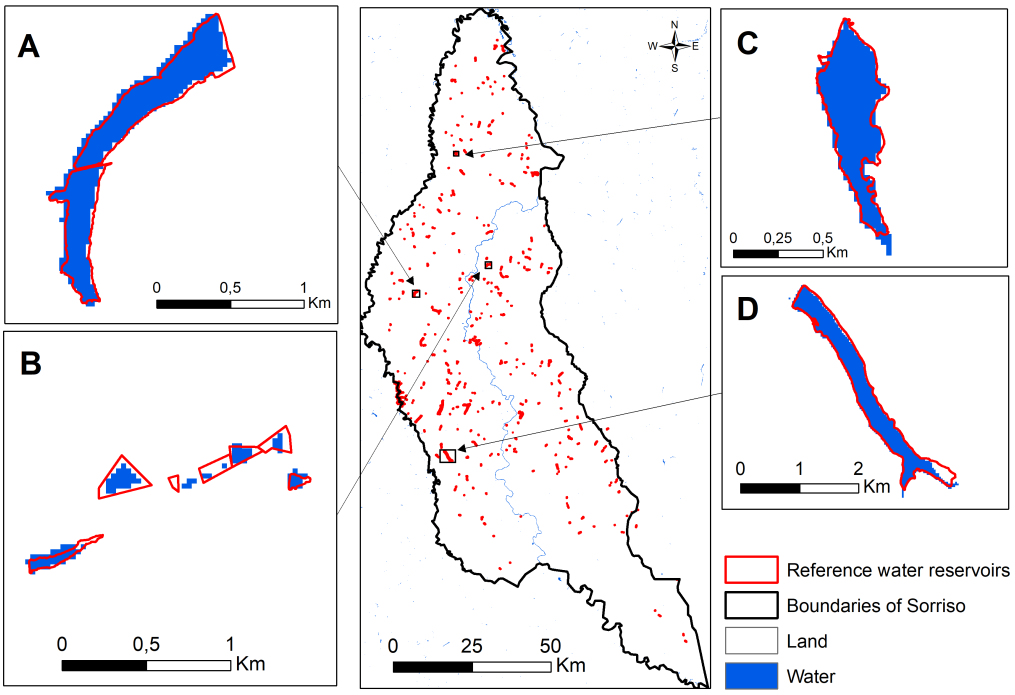

Figure 17: Maps of water bodies in Sorriso (MT) for year 2015.

changes have been dramatic for over 30 years, mainly due to deforestation. Many studies have used indicators to highlight climate changes in the Amazon. Data used are of four main types : in-situ measurements (raingauge and temperature stations), satellite data (mainly rainfall estimations), physical models (from global to regional scale, not presented here) and perceptions by local communities. There are some new challenges for using proxy data such as phenology, lake sediments or even palynology and dendrochronology but in the tropics, due to the lack of seasonal thermal contrasts, these methods are not so useful.

Many studies have used data from ground stations to characterized climate change. This is challenging in the Amazon because the climatological network is not very dense and many series have missing data. This leads to uncertainties about the effective trends about temperature and rainfall. Most of studies used statistical tests to detect the significance of trends or breaks in series (Pettitt, Mann-Kendal, Student among others). Results show a

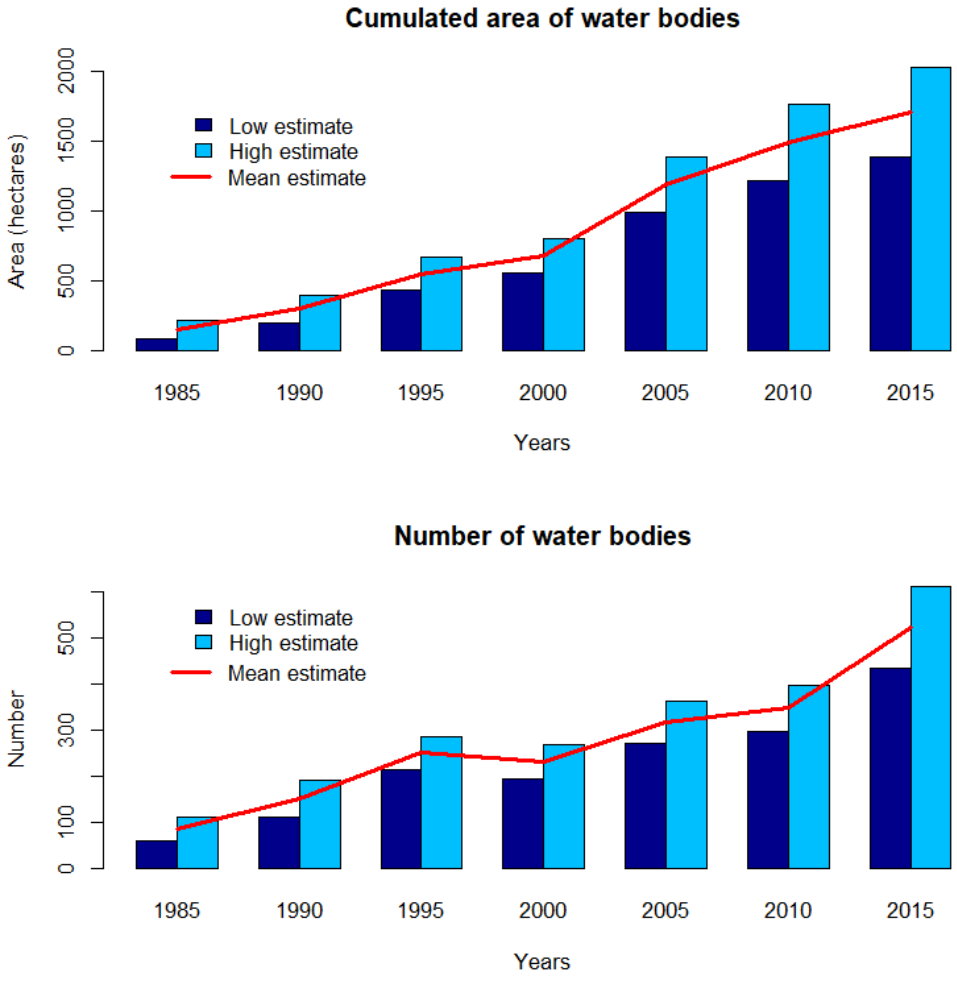

Figure 18: Temporal evolution of the cumulated area and number of water bodies in Sorriso between 1985 and 2015.

positive trend for temperature and a non significant trend for rainfall considering the whole Amazon. Some studies highlighted different trends between the south (negative) and the center of the Amazon Basin (positive). Using methods to detect the beginning and the end of the rainy season, some studies also showed some negative trends in the southern part of the region. More recent studies also used use the Kppen classification to evidence climate change in Brazil, not only looking at the shift between the averages of

two references periods but observing how each year (Annual Climate Types, ACT) can be classified using Kppen's method: the frequency of ACTs also showed a decreased of the rainy types in the South of the Amazon.

Satellite-derived estimates of precipitation are essential to compensate for missing rainfall measurements in the Amazon. These data have to be checked in order to detect any bias in replicating seasonal regimes or under/over estimating high/low intensities of rainfall. Moreover, there are few products that allow good rainfall trend estimations because of the short period of satellite observations. For example, the PERSIANN-CDR is a relatively new product (released in 2013) but that contains data since 1983, thus enabling long-term rainfall analysis. The computing of metrics for the rainy season (onset date, demise date and duration) on a pixel-to-pixel basis for each year in the time series allowed to identify significant trends toward a shortening of the rainy season in the southern Amazon, mainly linked to earlier demise dates.

Last type of studies concerns the perception of climate change using in-situ interviews of local communities, eventually comparing them with physical observed data. The results indicate that even if the perceptions are varied, and not always aligned with measured data, the arc of deforestation in southern Brazilian Amazon clearly shows an agreement of lower rainfall and higher perception of rainfall change by communities. Many times, however, the most striking element in open answers was the increase of the irregularity (or unpredictability) of rainfall. Both agricultural-based and traditional communities (that count on fishing, extractivism or family-scale agriculture) seem primarily sensitive to the interannual variability of rainfall.

2.4.1. Detection and attribution of rainfall changes by in-situ measurements

The climatological features of the Amazon Basin have been extensively detailed by, e.g., Marengo and Espinoza [46], Davidson et al. [47], Nobre et al. [48] and many others. The transition between the dry and wet season is primarily dictated by the onset of the South American Summer Monsoon (SASM) system, which in turn is controlled by large-scale thermodynamic processes involving the equatorial sea surface temperature (SST). The onset of the rainy season is established after the period of maximum seasonal temperature: During this dry period the atmosphere is very stable requiring a large increase in temperature and humidity at the earths surface to reach enough energy to create convection and instability. This increase in temperature acts to destabilize the atmosphere and cause a reversal in the horizontal

temperature gradients and vertical wind shear. While the onset of the rainy season takes place typically in a span of one month, the demise can take much longer. Interactions between land surface and the atmosphere, and particularly, between soil moisture and evapotranspiration, also work as dynamic mechanisms driving the remaining variance of hydrological processes on annual and inter-annual time scales in the Amazon. Changes in land surface (forest to pasture, agriculture and urban areas) also imply in strong physical modifications influencing the amount of available energy in form of latent heat and albedo inducing a stabilization of the CINE, in opposition to its reduction, engendering changes in the rainy season extend.

This complex set of various forcing, interweaving natural and anthropogenic actors brings up the question of whether precipitation patterns may be evolving in SA. Thus, in order to assess the regions precipitation regime during the last four decades of continuous deforestation (1971-2010), many authors focused their analysis in characterizing annual and seasonal climatic tendencies and ruptures at a regional scale, and also, climatic shifts as for the onset and offset of the rainy season and its length.

To accomplish this objective we have assessed data from 207 Rain Gauges (RGs) in both deforested and forested areas through two statistical parametric tests (Pettitt and Mann-Kendalls) and a linear regression analysis. In addition, we have identified the onset and offset of the rainy season, including its shifts and length based on methods proposed by Liebmann et al. [49]. Furthermore, we have used an ordinary exponential kriging interpolation analysis to map both linear regression and season onset and offset shifts. The regions natural climatic variability is discussed in light of these results. A second analysis using Mann-Kendall (MK) tendency test where values were assessed, considered the seasonal changes within the onset, offset and the rainy seasons length. This non-parametric MK statistical test is popularly used to calculate the significance of trend in hydrological time series. The test requires sample data to be serially independent. The test also allowed the assessment of the annual and seasonal historical rainfall patterns trends for the 1971-2010 period. In the seasonal analysis considering the onset and offset (LRA and MK), plus the rainy season length (MK) only 89 of the 207 RG were evaluated. These RG were selected because they were composed of more than 30 years of data.

The last methodology used in this study consists in using a buffer zone approach that correlates forest cover in each RG with rainfall trends for the 1971-2010 period. The areas analyzed comprise the Brazilian states of Mato

Grosso and Rondnia and their adjacent areas to the north, south, east and west. The buffers are delimited, merged and intersected using remote sensing and GIS techniques at local and regional scales. Each buffer zone is defined by: 1) a centroid given by the respective station coordinates, and 2) the surrounding neighborhood given by a circular area with radius from centroid equals to 1 km, 5 km, 10 km, 20 km, 30 km, 40 km and 50 km (roughly 7.850 km2 of total area for a 50 km buffer).

The 207 RGs analyzed depicted at least 2/3 of reduction in annual average precipitation depending on the analysis method. The tendency is significant for 94 RGs (45%) during spring and autumn months according to Mann-Kendalls monthly test, however, not significantly noticeable in the annual totals. The precipitation reduction in the rainy season is condensed in the onset and offset, affecting only modestly rainfall totals. These results were confirmed through the onset and offset analyses that indicated a strong contrast between the Amazon biome and the Cerrado.

RGs in deforested areas (more numerous in SA) indicated more negative than positive precipitation tendencies during the transition months. The onset-offset analysis suggested a reduction in rainy seasons length for more than 88% of the RGs in the 1971-2010 period, with a later onset and an earlier offset. The onset of the rainy season also revealed a heterogeneous pattern (late in the northwest of Rondnia and early in the MT and Xingus central-northeast areas).

Correlating buffer-zone-forest-cover and rainfall data demonstrates that at local level forest areas were not statistically correlated with the annual historical precipitation trends, but to some extend relevant to seasonal patterns (rainy season offset). In the Cerrado biome for instance, correlations are weak and do not show significance in 90% of cases. Albeit negligible in most cases, the correlations indicate that the larger the buffer area is, the greater the degree of correlation between land use and atmosphere. However, because this study was limited to remote sensing techniques and RG collected data, the authors cannot confirm that precipitation is correlated to forest cover changes in Southern Amazonia. The study is limited to suggest that large-scale deforestation may have a larger impact on precipitation distribution and the physics related to large-scale circulation dynamics in Southern Amazonia, particularly during the offset of the rainy season, which could increase the length of the dry season.

This study therefore also indicates that transitional zones of the Amazon biome (dense canopy) to Cerrado (savanna physiognomies: from woodlands

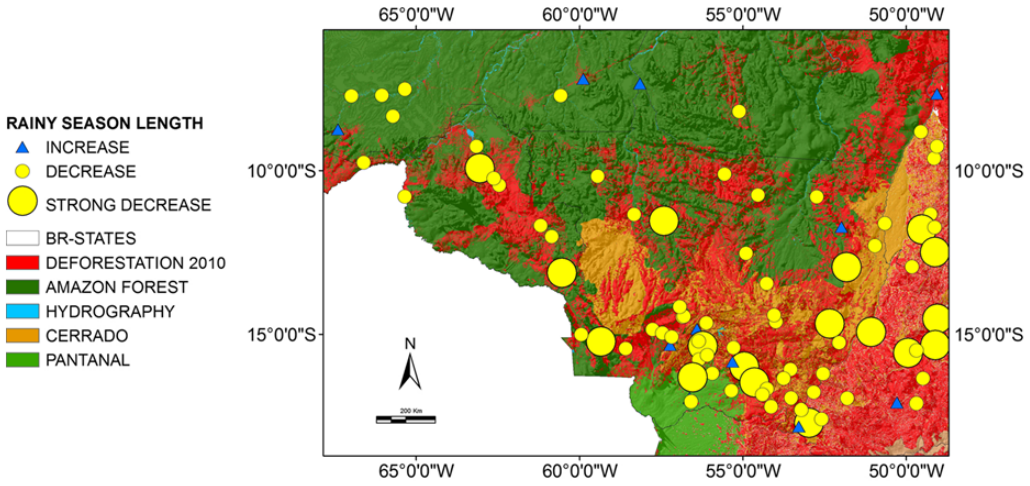

Figure 19: Tendency of the Rainy seasons length during 19712010. Small yellow circles represent the RGs with negative trends for the rainy seasons length; larger yellow circles represent a strong decrease in the rainy seasons length; blue triangles indicate positive trend within the rainy seasons length. There were no RGs depicting a strong increase in the rainy seasons length.

to open grasslands) imply in local particularities due to the physical implications of surface in the atmosphere. So, there is a great impact of the forest canopy on evapotranspiration, if compared to savanna areas in atmosphere-surface interactions; also, areas to the south of the case study region are more influenced by cold fronts with a smaller role of evapotranspiration during the dry season (winter).

Other variables not incorporated in this buffer study could ascent as strong indicators to be correlated with forest cover alone, such as evaporation rates or specific humidity. Also, despite of the numerous RG analyzed in this study, their location to the east and south of the case study (due to the recent context of colonization of the area) could mask data from stations placed in areas of rainforest and transitional forest (less numerous). In the future, a more extensive network of RG (when available) could more precisely test this hypothesis. It should also be relevant to compare the dry and rainy seasons as separated cases in forest cover and rainfall correlations.

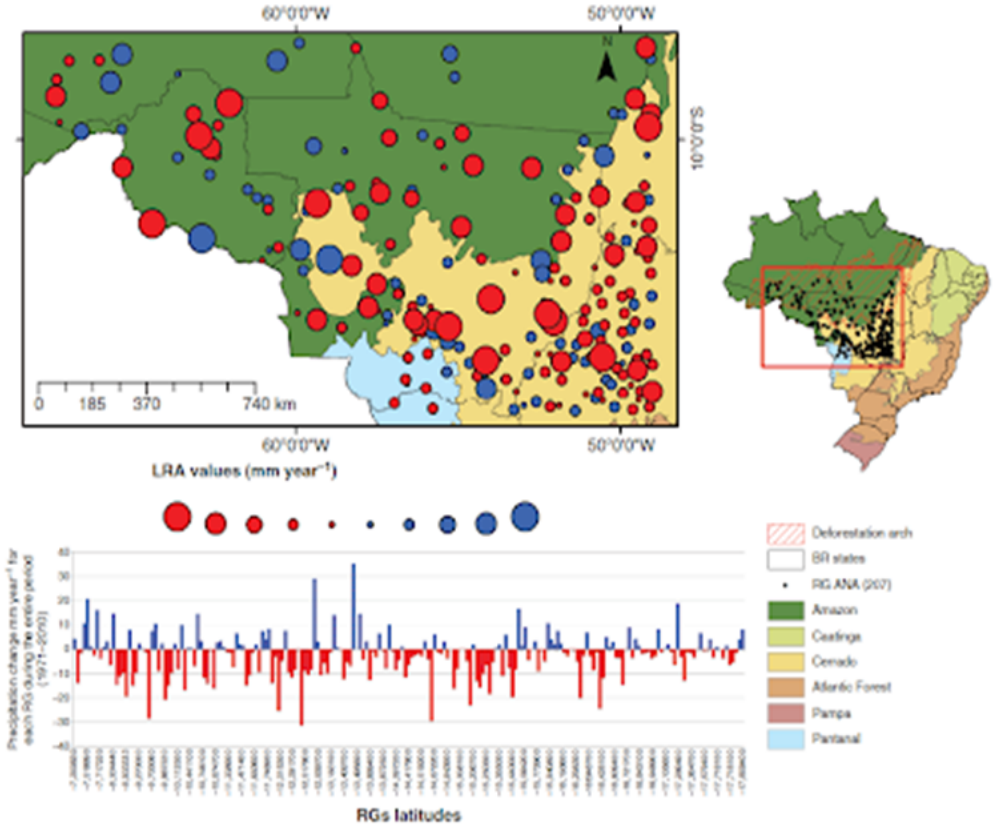

Figure 20: The map shows the distribution of precipitation change in the LRA analysis for 207 RGs. In the Brazilian map, the localization of the RGs within the biomes distribution is shown. In the left bottom graph, y-axis represents the precipitation change in mm according to the LRA for 207 RGs during the 1971-2010 period. The RGs are organized in the x-axis from the lower latitude to the highest. Blue represents the RG that had a gain in precipitation and red represents RG with a reduction in precipitation.

2.4.2. Indicators of the evolution of the rainy season by remote sensing

The Amazon region provides numerous essential ecosystem services, including food production, biodiversity conservation, carbon storage, hydrology and climate regulation. However, in the last decades, these services have been affected by the expansion of anthropogenic activities that threaten Amazonian ecosystems. The impacts of deforestation and agricultural development in the Amazon on local and regional climate are of particular concern. Khanna et al. Khanna et al. [50] suggested that deforestation is sufficiently

advanced to have caused a shift from a thermally- to a dynamically-driven climatic regime, which may affect the rainy season in the future. In this connection, previous studies have pointed to intensification of the dry season in the southern Amazon [51], and predicted intensification of rainfall during the rainy season or changes in the wet-day and dry-day frequencies.These predictions of climate change need to be confirmed (or refuted) using diverse datasets and methods to better assess the spatio-temporal patterns of precipitation in the Amazon.

In this context, remote sensing data are extremely important since they enable spatially and temporally homogeneous and continuous monitoring of rainfall regimes. The recent release of Precipitation Estimation from Remotely Sensed Information using Artificial Neural NetworksClimate Data Record CDR data (PERSIANNCDR), consisting of daily rainfall estimates from 1983 to the present, represents a great opportunity to both study precipitation patterns and to assess trends based on more than three decades of data as recommended by the World Meteorological Organization. We then used these data to assess changes in the rainy season in the southern Amazon since the early 1980s by computing four indicators of the rainy season : annual rainfall, onset date, demise date and duration.

These indicators were computed on a pixel-by-pixel basis for each hydrological year of the dataset (1983 to 2013 with the end of year 2013 occurring in 2014). The onset and demise dates and the duration were estimated based on a slightly modified version of the method proposed by Liebmann et al. [49]. Their method involves calculating a quantity called anomalous accumulation based on daily annual time series, which start 10 days before the driest month. The anomalous accumulation (AA) was calculated as in Equation 2:

$$AA(d) = \sum_{n=1}^{d} [R(n) - \bar{R}] \tag{2}$$

where d is the number of days, R(n) is daily rainfall and R is average daily rainfall. From this annual time series, the onset (demise) of the rainy season is defined as the day in which AA is minimum (maximum) (Figure 21). In the present method, unlike in the original method of Liebmann et al. [49], possible false rainy season reports were not considered. This simplified version presented less ambiguous values in the Amazon region. The duration of the rainy season consists in the number of days between the onset and the demise dates for each pixel.

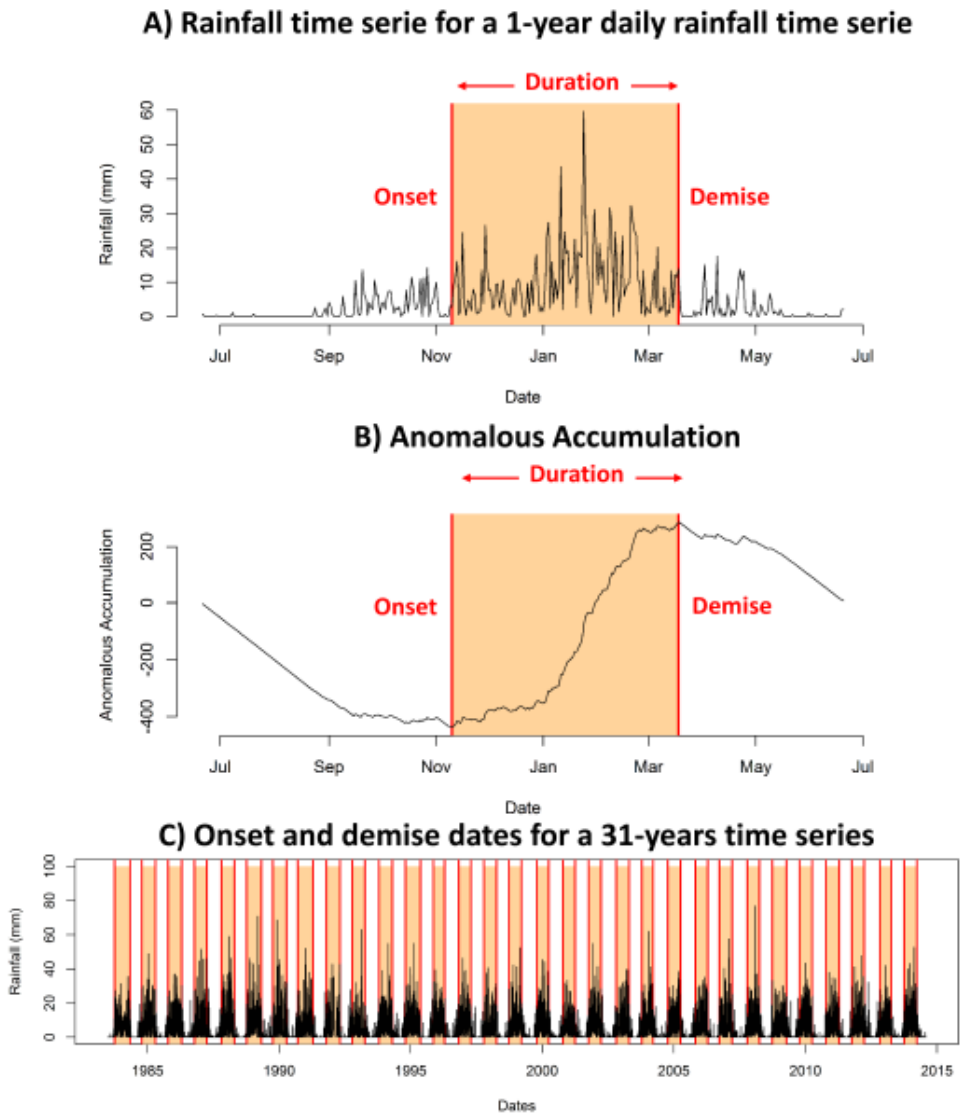

Figure 21: Illustration of the computation of the rainy season temporal metrics based on the method proposed by Liebmann et al. [33]. It includes: (A) a one-year daily rainfall time series for a given pixel; (B) the corresponding anomalous accumulation time series with identified onset and demise dates; (C) the entire (31-year) daily rainfall time series for a given pixel and its corresponding onset and demise dates.

In addition to the computation of the four indicators of the rainy season, we also calculated the averages and trends for each indicator of the rainy season computed over the 19832013 time period. Trends were computed based on the Mann-Kendall test. Here we present only the coefficient t of MannKendall, which varies from -1 to +1. The value of -1 (+1) indicates a trend of continuous decrease (continuous growth) in the study period. The value 0 indicates that there is no trend. Finally, a p-value of less than 0.05 was used to assess whether trends were significant.

The regions with the highest variability in annual rainfall are southern Par, southern Amazonas and Bolivia (Fig. 22, top left). The remote sensing estimates made it possible to highlight specific regions such as the Serra do Cachimbo in southern Par, which appears to be more rainy than the surrounding areas. The onset of the rainy season is earlier in northeastern Mato Grosso (MT) and southeastern Par (Fig. 22, top right). The beginning of the rainy season is later in western Mato Grosso (Chapada dos Parecis) compared to other areas of the same state. The differential onset of the rainy season across the state of Mato Grosso described here confirms previous observations and partially explains why double-cropping systems have been less widely adopted in this agricultural region (western Mato Grosso) than in central Mato Grosso. The demise dates follow a north-south gradient that is more pronounced than for the onset dates (Fig. 22, bottom left). Consistent with these results, the duration of the rainy season is longer in the north than in the south of the study area (Fig. 22, bottom right), with greater variability in Bolivia, along the Andean Cordillera, and in the southern and northern parts of the study area (not shown).

Concerning long-term changes in rainfall patterns, annual amounts tend to decrease regionally (Fig. 23, top left), although trends vary strongly in the study area and are mainly statistically insignificant, except for regions in Bolivia and western Mato Grosso. In addition, our results indicate positive trends for onset dates (delayed onset) in Bolivia and northern Mato Grosso (Fig. 23, top right), but they are mainly significant in Bolivia. Conversely, trends are negative (early onset) in the center of Mato Grosso and in Rondnia but are not significant. Trends in demise dates are significantly negative for the majority of the study area including southern Amazonas, parts of Acre and Bolivia, Rondnia, and western Mato Grosso (Fig. 23, bottom left), indicating a trend toward earlier demise of the rainy season in these areas. As a consequence, we also observed a trend towards a reduction of the length of the rainy season, with especially significant trends in Bolivia, Rondnia state

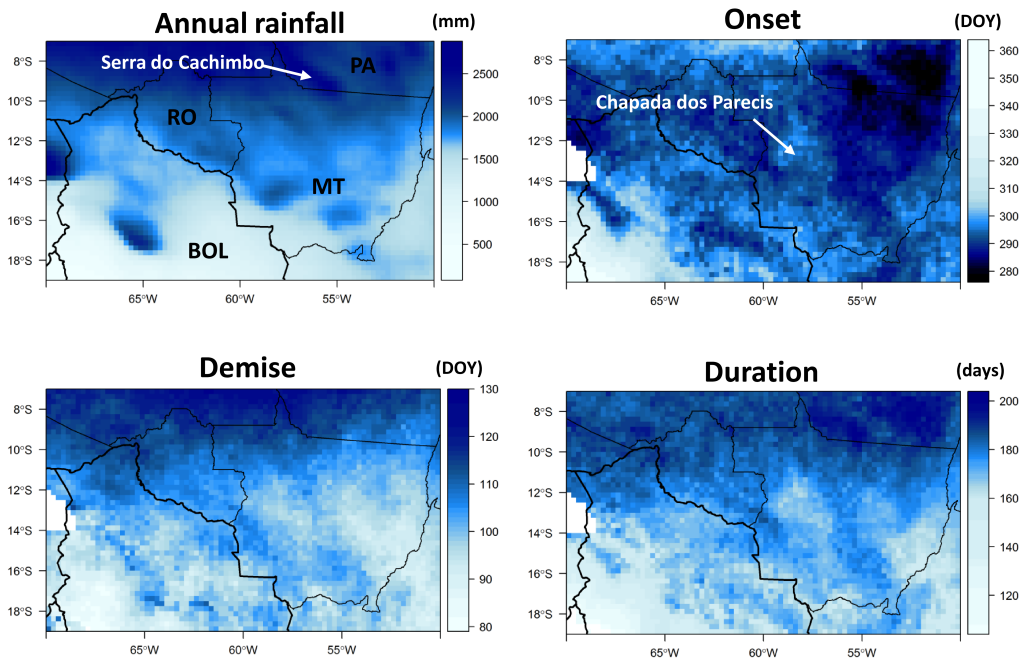

Figure 22: Mean annual rainfall, onset date, demise date and duration of the rainy season in the southern Amazon estimated from PERSIANN-CDR for the 1983-2013 time period. The onset and demise dates are defined as the number of days after January 1. Areas in white correspond to pixels where the rainy season is not well defined according to the Kppen classification rules. (PA = Par, MT = Mato Grosso, RO = Rondnia, BOL = Bolivia)

and southern Amazonas (Fig. 23, bottom right).

This work has been published in Arvor et al. [52]

3. Socio-environmental indicators

3.1. Deforestation vs socio-economic development

3.1.1. Deforestation vs income

In the late 2000s, seminal studies evidenced a boom-and-bust development pattern ([53, 54, 55]. That is, timber extraction and the conversion of forests into cropland and pasture generate a boom in incomes and jobs in the first years of land occupation, which is then followed by a collapse as

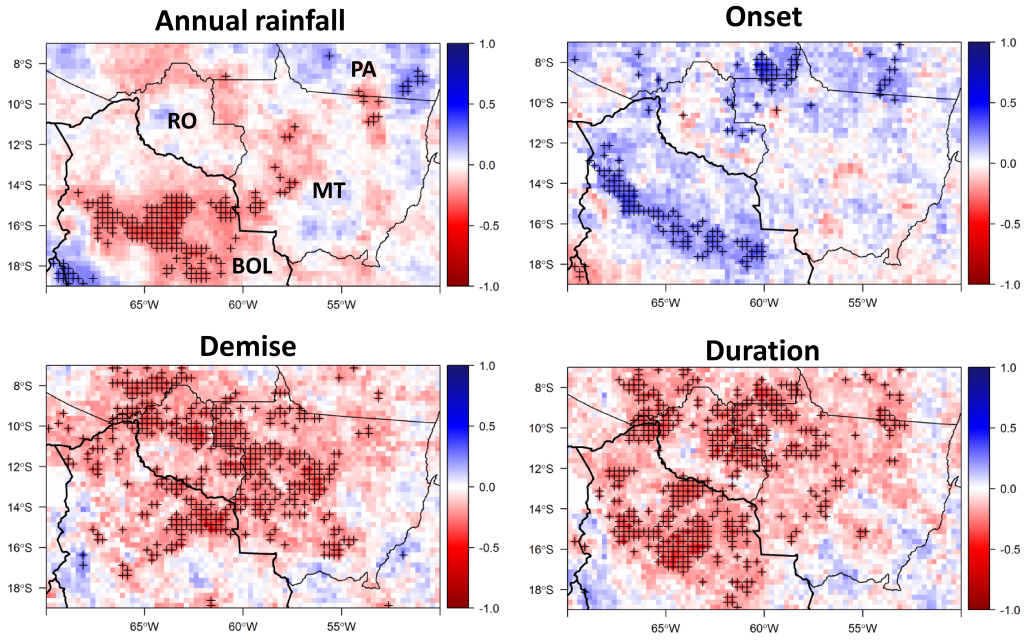

Figure 23: Trends in annual rainfall, onset date, demise date and duration of the rainy season in the Southern Amazon estimated from PERSIANN-CDR for the 1983-2013 time period. The trends correspond to the τ of Mann-Kendall. Significant trends are indicated with crosses. Areas in white correspond to pixels where the rainy season is not well defined according to the Kppen classification rules. (PA = Par, MT = Mato Grosso, RO = Rondnia, BOL = Bolivia)

forest resources and soil fertility are depleted [56]. Associated with high deforestation rates over the past four decades, the boom-and-bust pattern may be considered as a lose-lose scenario from a long term perspective since it generates high environmental costs and limited socio-economic benefits [57]. Yet, the last decade has been marked by a dramatic decrease in deforestation rates in the Brazilian Amazon [58, 59] and a significant increase in the Human Development Index (HDI) [60]. As a consequence, important recent studies reviewed the originally widely accepted boom-and-bust development hypothesis [57, 60]. While these studies provide evidence that deforestation has not been followed by a socio-economic decline and thus reject the boom-and-bust hypothesis in the Brazilian Amazon, they provide little insight into the current scenario of socio-economic development and deforestation across the Amazon.

To address this issue, we conducted a sub-municipal analysis of socio-economic development and deforestation in the Brazilian Amazon with the objective of providing evidence for the transition from a boom-and-bust to an EKC pattern in the Amazon. The EKC hypothesis predicts that environmental degradation may have an inverted U-shaped relationship with development: environmental degradation goes along with development until primary needs are met; then a turning point is reached when concerns for the environment increase and environmental degradation decreases [61, 62].

We crossed socio-economic data from full-population censuses in 2000 and 2010 provided by the Brazilian Institute of Geography and Statistics (IBGE) at census sector scale [63] with the PRODES deforestation maps provided by the Brazilian National Institute for Space Research (INPE) [64]. Both datasets were projected on a 10x10 km regular grid [65]. The final grid thus contains 30,693 cells for which we computed two deforestation indices also used by Rodrigues et al. [53]: (1) Deforestation extent is the cumulative proportion of deforestation in a cell in 2000 and 2010; (2) Deforestation activity is the proportion of land area in a cell that has been cleared during the preceding three years, i.e. 19982000 and 20082010 time periods.

In addition, we computed different measures of socio-economic development by referring to the standard of living (income per household in Brazilian Real, R$), literacy (proportion of literate heads of household) and access to basic services such as sanitation (proportion of households with toilets). To do this, we proportionally shared out the socio-economic data from each sector across all underlying corresponding cells.

While the boom-and-bust hypothesis analyses a pattern of socio-economic development depending on deforestation, the EKC explores how socio-economic development acts on deforestation. Concretely, we statistically tested the hypothesis of the emergence of an EKC in the Brazilian Amazon by measuring the relationship between deforestation activity and income per household based on a quadratic model (Eq. 3) where DEF is deforestation activity and INC is income per household. As suggested by Choumert et al. [66], we considered that an EKC relationship exists if the coefficient is positive for income ($\beta_1 > 0$) and negative for the squared income ($\beta_2 < 0$).

$$DEF = \beta_0 + \beta_1 INC + \beta_2 INC^2 + \epsilon \tag{3}$$

We then attempted to quantify the turning point of the EKC, i.e. the inflection point at which environmental degradation starts declining. We

thus focused our analysis on the identification of (i) an income threshold above which socio-economic growth does not appear anymore to be a driver of deforestation and (ii) a deforestation threshold above which new clearings do not appear to be a vehicle for economic growth. To identify the income threshold, we first sorted all cells according to income per household and grouped them by percentile. We then plotted the deforestation activity (in %) for each group of cells and computed a moving average in order to outline the trends. To ensure the best possible comparison between the 2000 and 2010 periods, we calculated the income per household relative to the Brazilian minimum wage (i.e. 151 R$ in 2000 and 510 R$ in 2010).

We measured the relationship between deforestation activity and income with Eq. (1). The results confirmed the hypothesis of a significant EKC relationship between income and deforestation (Table 1). Actually, we found an EKC for both 2000 and 2010, indicating that the transition to an inverted U-shaped relationship between deforestation and socio-economic development was already underway at the end of the 1990s, i.e. before the deforestation decline observed from the mid-2000s.

	2000	**2010**
β_1	0.985437***	0.322695***
β_2	-0.029710***	-0.040279***

Table 1: Coefficients of the quadratic regression model between deforestation activity and income for 2000 and 2010. *** indicates significance at the 0.1% level. We considered that an EKC relationship exists if the coefficient is positive for income ($\beta_1 > 0$) and negative for the squared income ($\beta_2 < 0$).

Then, the figure 24 depicts the deforestation activity as a function of income, and hence the EKC. It emphasizes a positive relationship between deforestation and income in low income areas. In the case of high incomes, the relationship is stable in 2000 and negative in 2010. For 2000, the curve does not illustrate the EKC hypothesis but the plateau explains why we statistically identified an EKC trend in 2000 (Table 1). In 2010, the inverted U-shaped curve is typical of an EKC and illustrates a decoupling between deforestation and socioeconomic development in the Brazilian Amazon as also expressed by Caviglia-Harris et al. [60]. Concerning the income threshold, in 2000, our results (Fig. 24) indicate an inflection point over an income per household equal to 2.5 times the Brazilian minimum wage, above which the relationship between income and deforestation reaches a plateau at high

levels of deforestation activity. In 2010, the turning point is observed around one minimum wage per household. Above this income value, deforestation activity decreased significantly. These results raise important issues about the relative responsibility of low and high income populations in explaining deforestation.

Finally, we defined a deforestation extent threshold using the ratio of the income per household in inactive cells (deforestation activity $< 0.5\%$) to active and very active cells (deforestation activity $> 0.5\%$) for different classes of deforestation extent. With this ratio, we aimed to identify a deforestation extent threshold above which the income per household in inactive areas becomes greater than in areas of active to very active deforestation. We focused the analysis on areas with deforestation extent values ranging from 10 to 90% since we considered that inactive cells are over-represented beyond these thresholds. To define classes in that range, we sorted the deforestation extent values for inactive cells (which are less represented in the database) and grouped them by percentile so that each class is represented by a fix number of at least N inactive cells and a variable number of K active and very active cells (K being usually greater than N). We then calculated the ratio between the median income per household in inactive cells and active + very active cells and outlined the trends with a moving average. Additionally, we also computed the ratio between the median income per household in inactive cells with the median income of the N richest and N poorest active cells (in terms of income per household) in order to (i) limit any bias related to over-representation of a class (in cases where K N) and (ii) define the full range of ratio values for each class of deforestation extent and thus provide a confidence interval to the results.

To define a threshold of deforestation extent, we analyzed the ratio between the median income in inactive cells (deforestation activity $< 0.5\%$) and active or very active cells (deforestation activity $> 0.5\%$) for different ranges of deforestation extent (Fig. 25). In 2000, low values (1) indicated no significant difference in income per household in areas undergoing active deforestation when compared with inactive ones, independently of deforestation extent. In contrast, in 2010, high ratios (>1) appeared for every range of deforestation extent so that the incomes per household were always higher in inactive areas than in areas undergoing active deforestation. So we cannot identify a deforestation extent threshold above which incomes in inactive areas become higher than in active areas. This assertion is even true when the ratio is computed comparing the income of all inactive cells with the

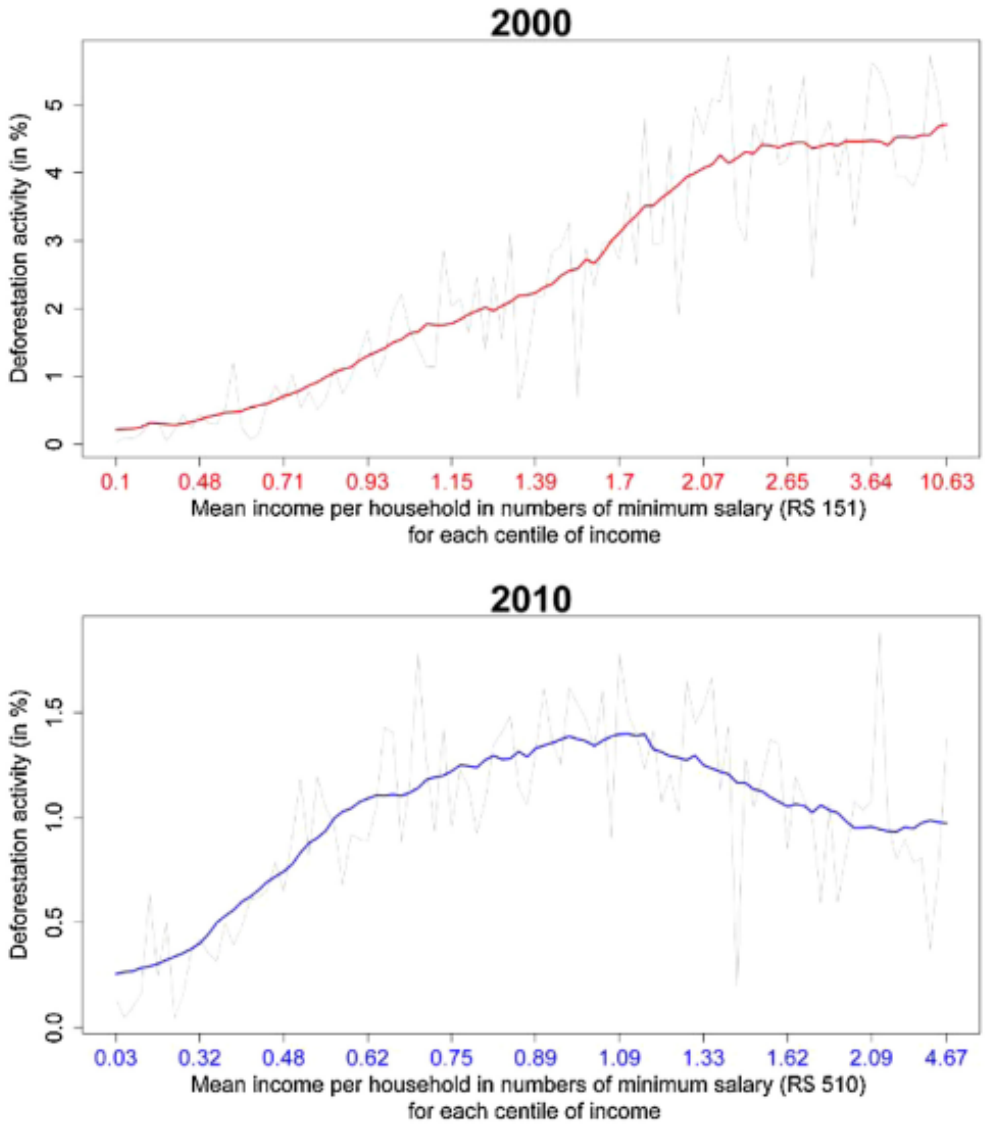

Figure 24: Deforestation activity as a function of mean income per household in 2000 and 2010. In 2000, the curve illustrates a positive relationship between income and deforestation activity. In 2010, this relationship follows an inverted U-shaped, evidence of the emergence of the EKC: beyond a income threshold of one minimum wage per household, deforestation activity begins to decrease.

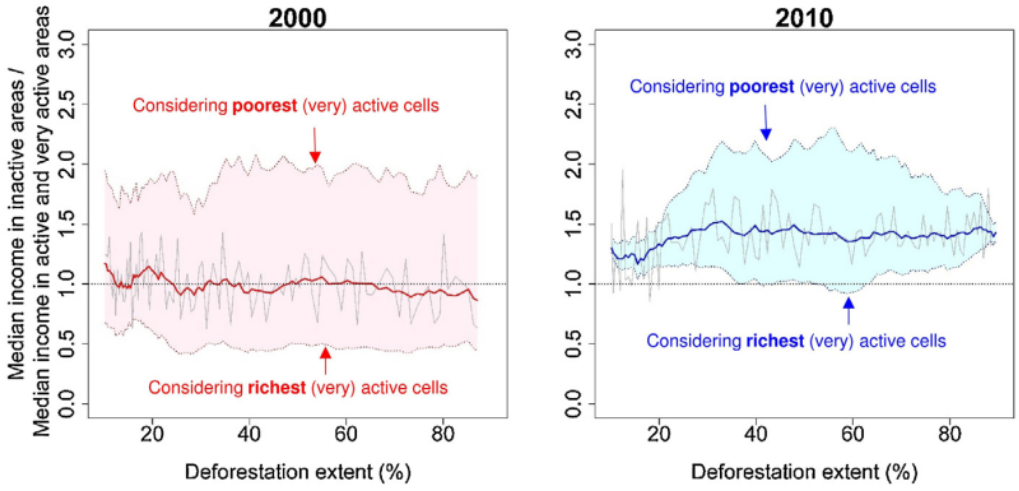

Figure 25: Ratio between the median income in *inactive* cells (deforestation activity <= 0.5%) and *active + very active* cells (deforestation activity > 0.5%) for different ranges of deforestation extent. High ratio values (>1) indicate that income per household in *inactive* cells is greater than in *active + very active* cells. Dashed lines represent the ratio between the median income per household in *inactive* cells with the median income of the n richest and n poorest *active + very active* cells.

richest active and very active cells only. This result is very important as it puts an end to the assumption that active deforestation is necessary to ensure socio-economic development in the Brazilian Amazon. Actually, it also emphasizes the importance of active deforestation as an indicator of a precarious economic situation.

This work has been published in Tritsch and Arvor [65]

3.1.2. Fragmentation analysis in Protected areas of the Brazilian Legal Amazon

Forest fragmentation and deforestation are a great concern in tropical regions, namely in South America and Africa, contributing to a rapid loss of tropical forest area with severe implications in ecosystem functioning and biodiversity conservation. One of the places with higher modifications in forest are the Brazilian Amazon, with the largest continuous region of tropical forest in the world. In the last twenty years, Brazil has been adopting land conservation policies, through the implementation of protected areas, in an

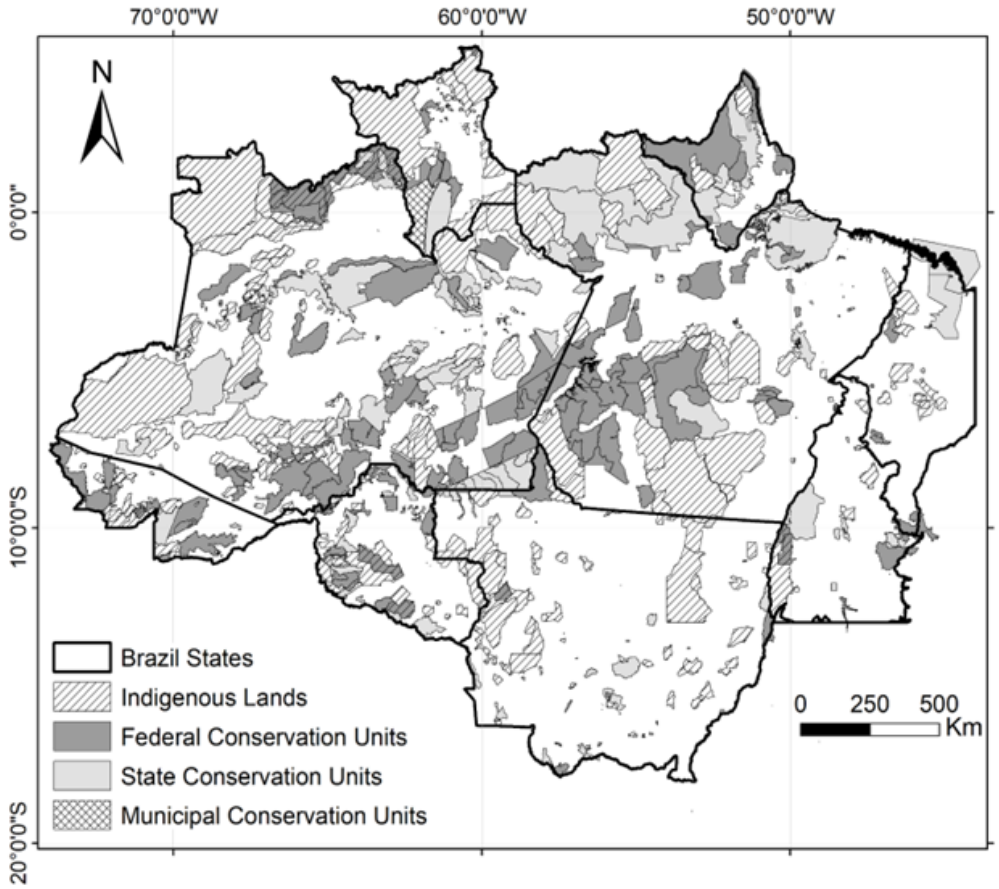

Figure 26: Protected areas located in Brazilian Legal Amazon.

attempt of preserving the remaining habitats and forests. Understanding the effectiveness of the created Protected areas (PAs) in reducing habitat fragmentation and deforestation is crucial to continue to implement these type of measures. We examined the effectiveness of PAs over the conservation of forest area in Brazilian Legal Amazon and to analyze patterns of deforestation inside and outside the Protected areas. In this regard, several landscape metrics were calculated and combined through statistic methods to build a landscape fragmentation index using remote sensing data at two-yearly intervals between 2002-2016. The research was conducted in all Protected Areas located (PAs) in Brazilian Legal Amazon (Fig. 26).

The calculated index was extremely important to have an idea of how PAs are effective in the conservation of forest ecosystem in the last fourteen years. Deforestation and fragmentation analysis revealed a trend of stability all over the study area with the exception of some hotspots, with an increase trend, in the arc of deforestation. Conclusions show that, despite some critical PAs, they contribute actively to improve the conservation of the native ecosystem and are extremely important, as political strategy, to reduce or avoid forest fragmentation and degradation processes. This work was submitted to a peer review journal and is currently under analysis.

We have also seeking an integrated analysis coupling forest fragmentation processes to income transfer programs and their effectiveness. The main question is "How can production alternatives be developed so that they ensure standing forest conservation, income generation and food security?". A preliminary analysis of a study case on the Uatumã Sustainable Development Reserve (Uatumã SDR) focused on the effectiveness of the Bolsa Floresta Programme (PBF), which is a state public policy introduced by the Government of Amazonas in 2007 aiming to the conservation of the forest through financial assistance to residents and community associations [67]. Within this programme, families can cultivate new lands only in the already cultivated ones to avoid primary forest deforestation and they receive a financial incentive equal to R$ 50,00 reais a month per family. Field work and interviews with local families showed their dissatisfaction with the programme. More detailed influence of the programme in the forest fragmentation process is under analysis.

This work has been published in Laques et al. [67]

3.2. Agricultural development vs life conditions

Land use sustainability in the Amazon is often approached from an environmental perspective [68], yet other dimensions of sustainability deserve to be better considered. On the one hand, we discuss how the rapid development of the agricultural sector in the Amazon frontier has brought major social advances, although it remains dominated by high social inequality, especially with regards to land tenure [69]. On the other hand, we argue that the recent trend towards agricultural intensification could lead to major health concerns which are still too rarely considered.

3.2.1. Towards a decoupling of soybean production and Human Development Index

In Mato Grosso, official statistics indicate a significant positive relationship between the Human Development Index (HDI) and soybean production at municipality level. The HDI increased continuously from 1991 to 2010, i.e. during the period of rapid frontier expansion, and remained higher in areas of soybean cultivation (Fig. 27, left). However, the HDI difference between non-soybean areas (i.e. municipalities where soybean production is null) and soybean areas is being reduced, as is also confirmed by the scatterplots relating HDI and soybean production (Fig. 27, right). Furthermore, a covariance analysis evidences that the linear models observed for each year (1991, 2000 and 2010) are significantly different, which may be interpreted as a decreasing influence of soybean production on HDI. These results thus indicate that, similarly to Macedo et al. (2012) who evidenced a recent decoupling between soy production and deforestation in Mato Grosso, HDI is also being decoupled from soy production, which could be the result of (i) efficient social policies promoted during the 2000s (Fome zero, Bolsa Familia, etc.; Hall, 2006) and (ii) the diversification of economic and agricultural activities which reduces dependency on a single commodity such as soybean. In this regard, this trend should be considered as a progress towards land use sustainability related to the consolidation of the Southern Amazon agricultural frontier. However, these results need to be validated in the long term. At the scale of the Brazilian Amazon, Rodrigues et al. [53] evidenced a boom-and-bust development pattern on the frontier: "relative standards of living, literacy, and life expectancy increase as deforestation begins but then decline as the frontier evolves, so that pre- and post-frontier levels of human development are similarly low". Indeed, development projects in the Amazon region traditionally have little scope for long-lasting development, despite being attractive to an extremely mobile and vulnerable population. Yet, the boom-and-bust hypothesis in the Amazon has recently been contradicted. Commodity-based agricultural activities on the Southeastern Amazon agricultural frontier may actually reverse the trend towards a bust pattern, through the accumulation of wealth, the establishment of intensive commercial activities and the reinforcement of local institutions that may warrant long term economic and social development. Nonetheless, the last (2005-2006) fall in commodity prices that caused a two-year decrease (2006-2007) in soybean cultivated areas in Mato Grosso emphasized the latent weaknesses of the current agricultural

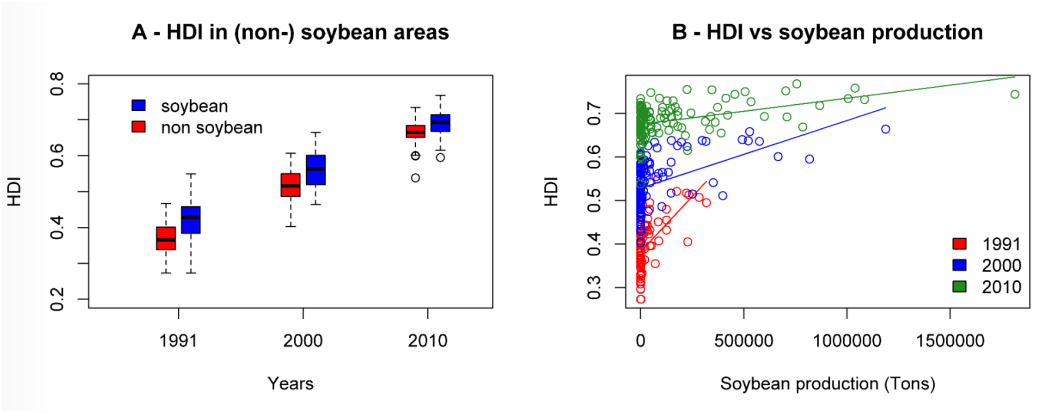

Figure 27: Evolution of the Human Development Index (HDI) at municipality level in Mato Grosso. (A) Comparative evolution of the HDI in soybean and non-soybean municipalities in 1991, 2000 and 2010. (B) Scatterplots relating HDI to soybean production at the three same dates. The pairwise nested model comparison F-tests all led to p-values ¡ 4.10-4 (source: soybean production; Human Development Index).

model, especially with regards to the indebtedness of farmers [70].

This work has been published in Arvor et al. [71]

3.2.2. Agricultural intensification: a threat to human health

The recent land use changes also raise major health concerns. Actually, a new epidemiological profile emerged during the last decades (Fig. 28). While the first stages of deforestation promoted epidemics of vector-borne diseases, such as leishmaniosis and malaria, due to the contact with vector's ecological niches, the subsequent conversion of wildlands to large single crop areas reduced the incidence of such diseases, especially in Northern Mato Grosso where new cases of malaria decreased drastically. On the contrary, violence, which is partially expressed by homicide rates, arose quickly in the end of 1990's. The expansion of the frontier was accompanied by illegal appropriation of land parcels, conflicts with indigenous and other traditional population groups, and rapid urbanization promoted by the expulsion of rural population to city peripheries. After a rapid increase during the 1990's decade, homicide rates have stabilized at high levels. Moreover, cancer mortality rate rose steadily in Mato Grosso state since 1995, due to genetic, demographic and nutritional conditions but also potentially because of high

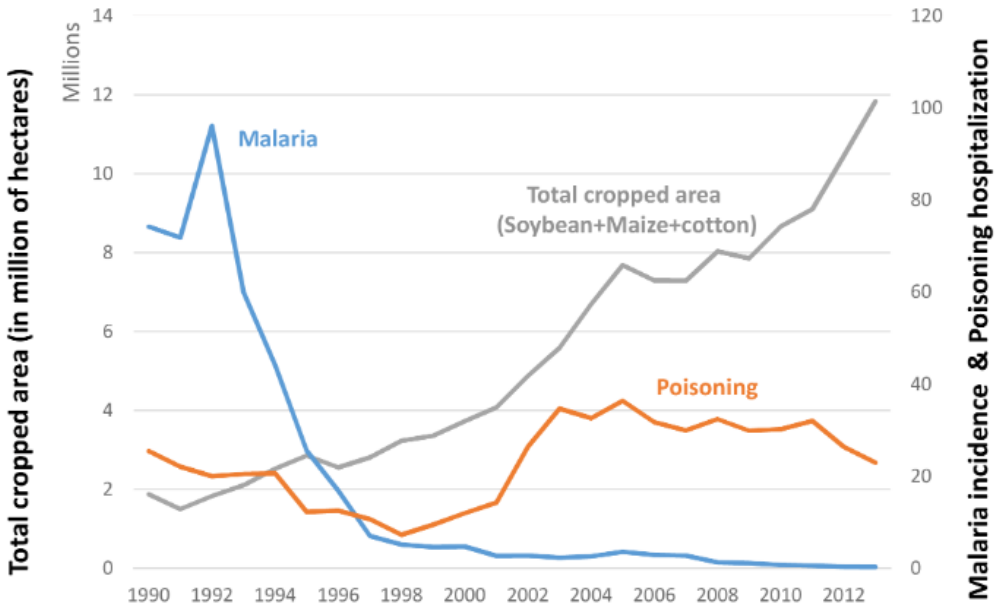

Figure 28: (A) Malaria incidence in Mato Grosso, according to the Annual Parasite Index (API-SIVEP), calculated as the number of positive blood slides per 1000 inhabitants, and cancer mortality and homicide rates, expressed by the number of deaths per 100,000 inhabitants (SIM), and (B) Hospitalization rates in Mato Grosso, calculated by the number of hospital discharges due to poisoning events per 100,000 inhabitants (SIH), and suicide attempts using agrochemicals as registered by the health notification system (SINAN).

level of exposure to agrochemicals as it has already been evidenced in other areas of intensive agriculture.

As mentioned previously, the use of agrochemicals increased rapidly in the last decades to support the agricultural intensification process and the diversification to maize and overall cotton crops in Mato Grosso. Considering that (i) Brazilian farmers are still allowed to use large amounts of agrochemicals banned in other countries, mainly in Europe and the United States, and (ii) applications are often carried out by plane, it raises important health issues such as acute poisoning and other diseases caused by chronic exposure to agrochemicals for populations working and living in intensive agricultural areas. First studies led in the neighboring state of Mato Grosso do Sul evidenced a close relationship between crop production and health exposure issues. The role of insecticides such as organophosphates and carbamates as

a main cause of human intoxication occurring in crop fields has been pointed out. Such studies should now be applied to other states such as Mato Grosso where the situation is quite worrying and needs to be better considered to take into account the social dimension of land use sustainability. Poisoning became a threatening health problem in Mato Grosso, as revealed by the occurrence of hospitalizations due to poisoning, which increased sharply in the early 2000s (Fig. 22B). The occurrence of an annual mean of 100 notifications of poisoning due to the exposure to agrochemicals, and 860 hospitalizations due to poisoning in the recent years (2010-2013) are worth of concern. This data is certainly underestimated as, according to the Health Ministry, for each recorded case of poisoning notification, other fifty were not registered. Water and soil contamination, air pollution due to biomass burning (forest and plantation) and temporary crop production were associated with the large use of agrochemicals in the cerrado biome. Similarly, while some studies have evidenced the depressive effects of agrochemical exposure that can lead to suicide, it has been observed an increase in the number of suicide attempts using agrochemicals, varying from five cases per year in 2000 to over fifteen in the 2010s.

This work has been published in Arvor et al. [71]

3.3. Agricultural practices vs climate conditions

The scientific community is questioning (1) the impact of human activities on climate, (2) what drivers lead to the development of human activities in the tropics and (3) how societies adapt their activities to climate change. Here, we focus on this last question to assess how climatic conditions affect choices made by farmers. Providing efficient responses to such issue first requires overcoming scale issues for linking anthropogenic dynamics to climate trends. Indeed, human activities are usually monitored at local or regional scales whereas climate trends, especially in the tropics, are considered at regional scales due to difficult access to realistic information on the spatiotemporal distribution of rainfall regimes because of heterogeneous sparse raingauge networks and frequent missing data in historical series.

Here we correlate metrics of the rainy season observed by remote sensing data with agricultural dynamics observed with MODIS-derived agricultural maps in order to assess how climatic conditions affect choices made by farmers.

We crossed (1) agricultural maps introducing singe and double cropping systems produced based on MODIS EVI time series with (2) maps of metrics of the rainy season (e.g. total rainfall, onset, demise and duration) produced with TRMM 3B42 data. We then calculated the proportion of double cropping systems per 3B42 pixel (0.25 ° 0.25 °).

The results (Fig. 29) clearly indicate that the higher proportion of double cropping systems is observed in areas characterized by high annual rainfall (¿1900 mm) and a long rainy season (¿180 days). The onset of the rainy season also appears to be important. Where the onset occurs before 16 October, the proportion of double cropping systems exceed 45% of cultivated areas whereas this proportion is below 30% in other areas. In the same way, areas where the end of the season occurs before 30 March, show low proportion of double cropping systems (<20%). These temporal thresholds are in total agreement with information collected during surveys with local farmers who estimate that the second crop cannot be sown after 18 February. Considering that the average soybean crop cycle lasts 120 days, it means that the last day for sowing the first crop of soybean in a perspective of adopting a double cropping system is 18 October. However, there also exist soybean varieties with short crop cycles (up to 90 days) that explain why the double cropping systems can still be adopted (around 30 %) even in areas where the onset of the rainy season occurs later.

3.4. Climate Change perceptions by Amazonian Communities

In the Amazon region lives an heterogeneous population consisting of ancient Amerindian and traditional communities, exploiting forest and river resources, as well as migrants from the pioneer front that transform rural areas and develop new urban centers. However, living conditions remain precarious especially in rural areas despite rapid economical development, and environmental impacts continue to increase; thus the overall sustainability of the Amazon remains questionable. The magnitude of changes in Amazonia deforestation, agricultural colonization, soil erosion and biodiversity loss has highlighted issues related to the regions sustainable development strategies.

The changes are both global and local and people try to balance their lifestyles and territorial development with the changes observed or perceived in their environment. In general, a perception of change is a first, necessary step to adaptation [72], thus developing adaptation strategies to climate change implies to understand how populations perceive and use their environment. In the Amazonian context, many communities depend on the

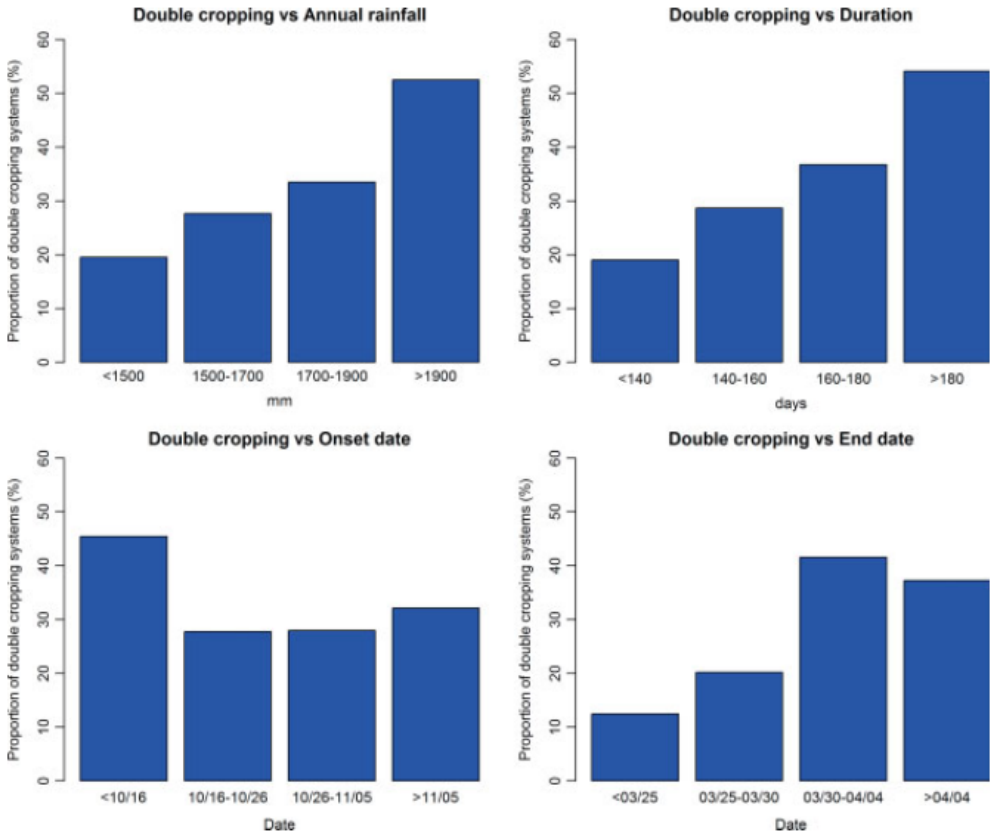

Figure 29: Relations between rainfall metrics and the proportion of double cropping practices at local scale, i.e. for each 0.25 ° 0.25 ° cell equivalent to a 3B42 pixel.

rivers for their livelihood at several levels, and are thus more vulnerable to pronounced variations in precipitation and water levels. Indeed, environmental perceptions have an intrinsic value that reveal the culture and local wisdom, and is crucial for public policy, environmental management, and for the definition of adaptation strategies related to climate change, as recognized in the Paris Agreement (COP-21 Article 7.5).

In this context, the Duramaz project (2005-2010) initiated an original pro-gram to qualify and quantify sustainable development for selected sites in the Amazon using indexes to measure the degree of socio-economical development and environmental commitment. 12 locations that reflect the diversity of social, ecological and economic situations across the Brazilian

Amazon were chosen as study sites. In each location, in-depth studies were conducted, including the collection of a vast array of socio-economic data at site, household and individual levels.

In this study, we combine quantitative and qualitative data to examine observed rainfall patterns and the perception of their changes by populations in these communities. We seek to identify key indicators of the perception of climate dynamics and its evolution by the population, through the surveys conducted with local populations. By comparing the observed, physical data with the perceptions by the local communities, we aim at a better understanding of how these populations perceive their environment, and by what preeminent climate indicators they evaluate their habitat and support social and economical decisions.

In this work we use the daily rainfall estimates from the Precipitation Estimation from Remotely Sensed Infor-mation using Artificial Neural Networks Climate Data Record (PERSIANN-CDR) to derive trend estimates for gridpoints nearest to the study site. (See paragraph before)

The DURAMAZ research project conducted extensive fieldwork in each of the selected sample sites. Of the 12 sites used in this study, six correspond to family-scale agriculture (Anapu, Parauapebas, Alta Floresta, Ouro Preto do Oeste, Juna) or agrobusiness (Sorriso) sites, five are traditional communities located within protected areas (Iratapuru, Mamiraua, Tup, Ciriaco, PAE Chico Mendes), and one is an amerindian village within a protected area (Moikarako). A massive amount of socio-economic quantitative data have been collected through three questionnaires which were each applied at a given scale. Nearly 900 households were interviewed between May 2007 and August 2008 representing about 1250 accumulated days of fieldwork across all sites. At the site level, the most relevant stakeholders were surveyed on the issue of governance and institutional aspects. At the house-hold level, socio-economical data were collected on household composition and income, agricultural production, schooling, transport, consumption, etc., with a total of 110 variables. It also included a number of questions about the perception that local population had about the environment and the ongoing changes they were witnessing (or not). Finally, at the individual level, life-history questionnaires gave a wealth of data about the trajectories of the people who compose the contemporary local communities. For each site, interviews were conducted under a sampling scheme. When the site had less than 75 families, every household was surveyed. Otherwise, a random sampling was realized to conduct 75 interviews, with the verification by the survey team that all

parts of the studied area were represented in the sample. In each household, the chief of family was interviewed.

An indicator system was then derived from those data to obtain a view about sustainability and governance issues. It was composed of four main modules (living conditions; environmental conditions; needs of the present and future prospects; governance) and built on 44 sub-indicators derived from the questionnaires. The present study exploits the results of question 70-71 of the household questionnaire in which the family head was asked about his/her perception of climate change over recent years. The questionnaire allowed the following responses for question 70: changes in the dates of the harvests, changes in rainfall cycle, increase of the dry seasons length, the climate is warmer, the climate is colder, the winds changed, no change, other. The respondents could choose between one or more answers. Question 71 was used in order to detail the answer in case it was other, and any comment in relation with climate change perception.

The most frequent response (58% of respondents) pointed to a perception of a warming climate, against 3% of responses indicating a colder climate and 20% no change. These variations can be attributed to the observation of effectively warmer conditions, but since the spatial distribution of responses shows no obvious pattern, it could be that the responses were either induced by the question itself or partly conveys the influence of the media coverage on climate change. Indeed, interviews conducted by another Brazilian research team show that such perception is shared by the majority of smallholders in all biomes of the country. Unfortunately it was not possible to have a long-term in-situ temperature measurements on all of our study sites, and no such data is available from satellite measurements, therefore we show results from the analysis based on trends in rainfall.

Comparing physical quantities (often considered as objective) with social data on perceptions constitutes a challenge. Several bias must be taken into account: Differences in the nature and date of establishment of the communities as well as generational effects were all considered within the protocol developed in the project DURAMAZ. Thus, the statistical analysis provides the proper representation of the collected answers.

We are mostly interested in the perceptions related to precipitation, which appear as significant for about 35.2% of the interviewees. Nearly all answers related to changes in rainfall indicate perception of decrease in rainfall volume, stronger intensity, and most frequently lengthening of the dry season (12.6%). These results are in general agreement with the overall trends ob-

served in the Amazon: precipitation pattern changes are less clearly perceived than those of temperature, and that is linked to (i) the greater spatial and temporal variability of rainfall and a less clear signal of its trends across the basin, and (ii) lesser imprint of any debate on climatic change regarding rainfall. Narrowing the analysis into detail, the perceptions of changes by the communities are varied and the agreement with the satellite observations are not always good.

Our results indicate that even if the perceptions are varied, and not always aligned with measured data, the arc of deforestation in southern Brazilian Amazon clearly shows an agreement of lower rainfall and higher perception of rainfall change by communities. Many times, however, the most striking element in open answers was the increase of the irregularity (or unpredictability) of rainfall. Both agricultural-based and traditional communities (that count on fishing, extractivism or family-scale agriculture) seem primarily sensitive to the interannual variability of rainfall.

This work has been published in Dubreuil et al. [73]

3.5. Health-environment indicators

3.5.1. Indicator of landscape contribution in the exposition risk to malaria vectors

Despite the successes since 2000 in reducing both incidence and mortality of malaria worldwide, the disease is still highly present, with 216 million (95% confidence interval [CI]: 196263 million) cases and 445,000 deaths worldwide in 2016 (WHO, 2017). Moreover, local recrudescences of cases have been noticed in 2016 and 2017, especially in the Americas. Despite the WHO region of the Americas had recorded a 22% reduction of the incidence rate between 2010 and 2016, the same region recorded a 36% increase of the incidence rate between 2015 and 2016, especially due to increases of case number in Brazil and Bolivarian Republic of Venezuela (WHO, 2017).

In South America, the Amazonian region gathers the majority of malaria cases. Deforestation in the Amazon rainforest has been identified as a significant factor of malaria risk. Stefani et al. [74] carried out a systematic review and formalized the elements of consensus regarding the relationship between malaria transmission by the main malaria vector in this region, Anopheles darlingi, and deforestation in a knowledge-based model: (i) deforested areas can supply favorable conditions for malaria vector breeding

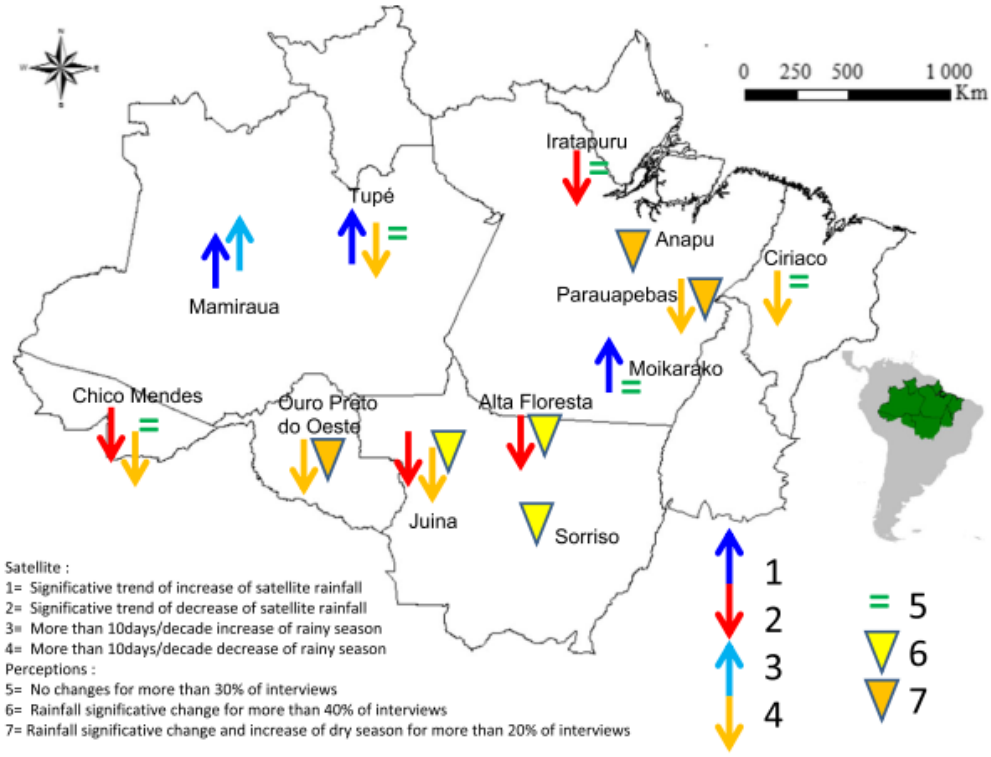

Figure 30: Synopsis of perceptions of rainfall changes for the studied sites.

and feeding because they are usually accompanied by the presence of human populations and activities; and (ii) forested areas can provide resting sites for adult vectors that return to forest after their blood-meal in deforested areas. Based on such a knowledge model, an indicator, called Normalized Landscape-based Hazard Index (NLHI), was built to evaluate the dangerousness of the landscape, all other things (especially vector presence and density, human population presence and density, individual behaviour, etc.) being equal.

The NLHI was defined as the linear normalization of the product of two landscape metrics: i percentage of forest (pF) and ii) forestnon-forest edge density (ED), both computed within a discoidal moving window with a radius of 400 m. Such a radius has been identified as the most significant in order to explain malaria incidence rates by Land Cover Land Use (LCLU) and LCLU-based landscape features [75].

A R program for NLHI computation from TerraClass (INPE) product

has been developed and will be made available online. It was applied and validated in the cross-border area between French Guiana and Brazil, using a 10 m spatial resolution forest vs. non-forest land cover map derived from SPOT 5 multispectral imagery. In a second time, the index was implemented at a larger geographic scale using a 30m spatial resolution Forest - Non forest map derived from the TerraClass product from the Instituto Nacional de Pesquisas Espaciais (INPE).

Notably, NLHI tends to explain more than 60% of the incidence rate variance (R2=0.63, p-value <= 0.001) at a local scale, in an area where other risk factors are supposed to be relatively uniform (thus preventing to generalize such a result to larger geographic scales or more heterogeneous contexts). At larger scale using a 30m spatial resolution Forest - Non forest map, the NLHI did not exhibit significant performance loss.

This work has been carried out as contributions of other projects: GAPAM Sentinela (Guyamazon), TlPal (CNES/TOSCA).

This work has been published in Li et al. [76] and Li et al. [77]

3.5.2. Epidemiological indicators : An Operational tool for malaria at the French-Brazil cross-border region

The number of malaria cases drastically dropped worldwide between 2000 and 2015, with 58% and 37% decreases of the mortality and incidence rates, respectively. Such a success conducted, in 2015, the statement of an ambitious target in the framework of the Sustainable Development Goals of the United Nations: By 2030, end the epidemics of [...] malaria [...]. However, several obstacles make actually such a target difficult to reach. First, malaria is still highly present worldwide, with 216 million cases and 445 thousand deaths worldwide in 2016 (WHO, 2017). Secondly, local recrudescence of cases have been noticed in 2016 and 2017, especially in the Americas. Particularly, Brazil notified 174,522 cases between January and November 2017, i.e. 56690 cases more than for the same period in 2016, representing a 48% increase (PAHO, 2018). Moreover, specific contexts favour the maintenance of foci of intense transmission. Particularly, cross-border malaria is considered as a major obstacle for elimination. In fact, on either side of the border, different public policies and different strategies and means of surveillance, prevention and control of diseases coexist, without regular exchange of comparable data and information, within socio-demographical and environmental contexts that already vulnerabilize the local populations. Such a

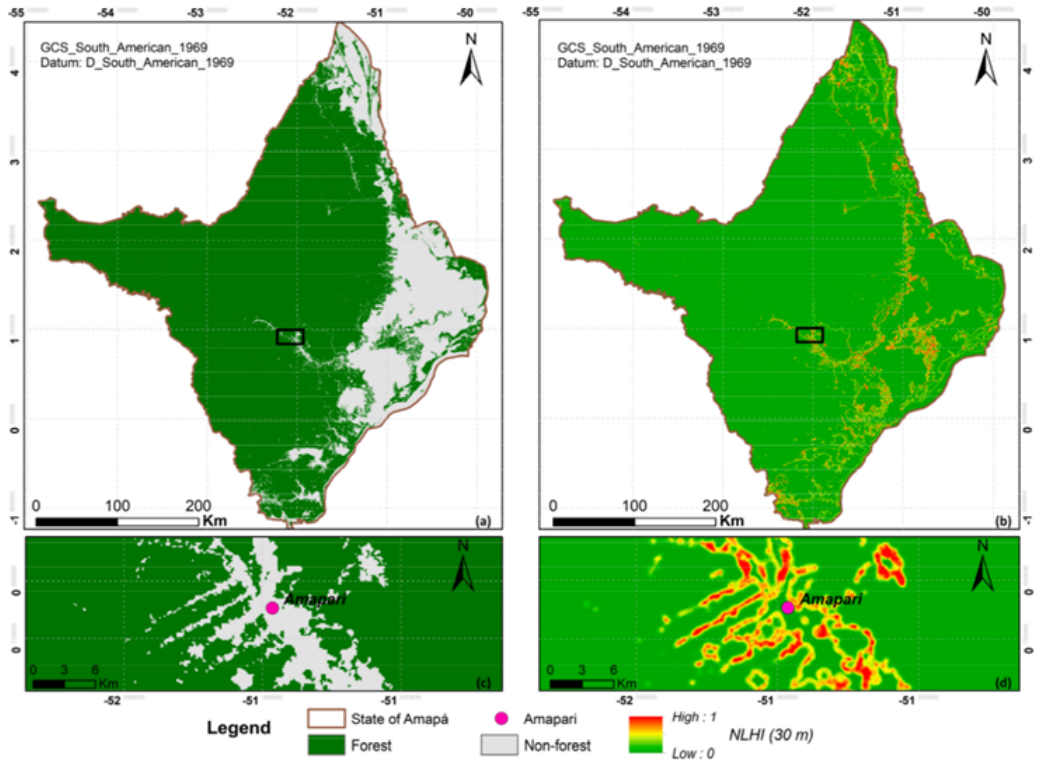

Figure 31: Results of large-scale NLHI computation. (a) Forest - Non-forest map in the State of Amap; (b) NLHI map of Amap state; (c) Zoom of Forest - Non-forest map near Amapari, Amap state; and (d) corresponding NLHI values near Amapari.

situation prevents to have a shared and unified vision of the epidemiological cross-border situations and, consequently, to define concerted (between the border countries), targeted and effective control actions.

Transform malaria surveillance into a core intervention is one of the three pillars on which the Global Technical Strategy of the World Health Organization (WHO) bases the actions towards the disease elimination. However, surveillance remains a challenge in cross-border contexts due to above mentioned issues, making necessary the harmonization of data types and formats, nomenclatures and concepts used by each country.

The border between French Guiana and Brazil is typical of the above described cross-border contexts. Systematic, regular and perennial information and data exchange related to malaria cases does not exist yet. Consequently,

a system for automatically integrate, harmonise and visualize cross-border malaria data has been built, in the framework of the Brazilian Climate and Health Observatory.

This system is fed by the existing country-specific surveillance systems: the Epidemiological Surveillance System for Malaria (SIVEP-Malria) in Brazil and the epidemiological surveillance system of the department of Delocalized Centres for Prevention and Care (CDPS) of the Cayenne hospital, French Guiana. It relies on expert knowledge in parasitology, epidemiology, national surveillance systems and informatics in order to specify data transformation rules leading to cross-border harmonized information. Nomenclatures chosen satisfy as far as possible international standards. Extraction, Transform and Load (ETL) tools were used in order to implement the rules and build a database containing harmonized information and shared by the two countries. Data visualisation tools implemented within the R-Shiny programming environment permit to disseminate the harmonized epidemiological indicators online, both temporally (time-series) and spatially (maps). Eventually, this system aims at being operationally implemented, for use for research works, epidemiological surveillance and general public information.

An operational version of the integration, harmonisation and visualisation system is due to late october 2018. Its operational deployment is conditional on first obtaining the authorization of the French regulatory commission (Commission Nationale Informatique et Liberts, CNIL) relative to the automatized processing of personal data, which has already been requested. Access to the system will be done through the website of the Climate and Health Observatory (Fiocruz) that hosts the cross-border Sentinel site at the French Guiana - Amap border (https://climaesaude.icict.fiocruz.br/amapa-guiana-francesa, en construction).

This works has been partly implemented under the frame of the GAPAM Sentinela (Guyamazon) project, Fighting Malaria: from global war to local guerrillas at international borders (OPP1171795, Grand Challenges Explorations Round 18, Phase I, Bill and Melinda Gates Foundation)

This work has been published in Roux et al. [78]

4. Conclusion

In this document, we introduced a list of indicators produced by the WP3 team of the ODYSSEA project. These indicators enable to monitor environ-

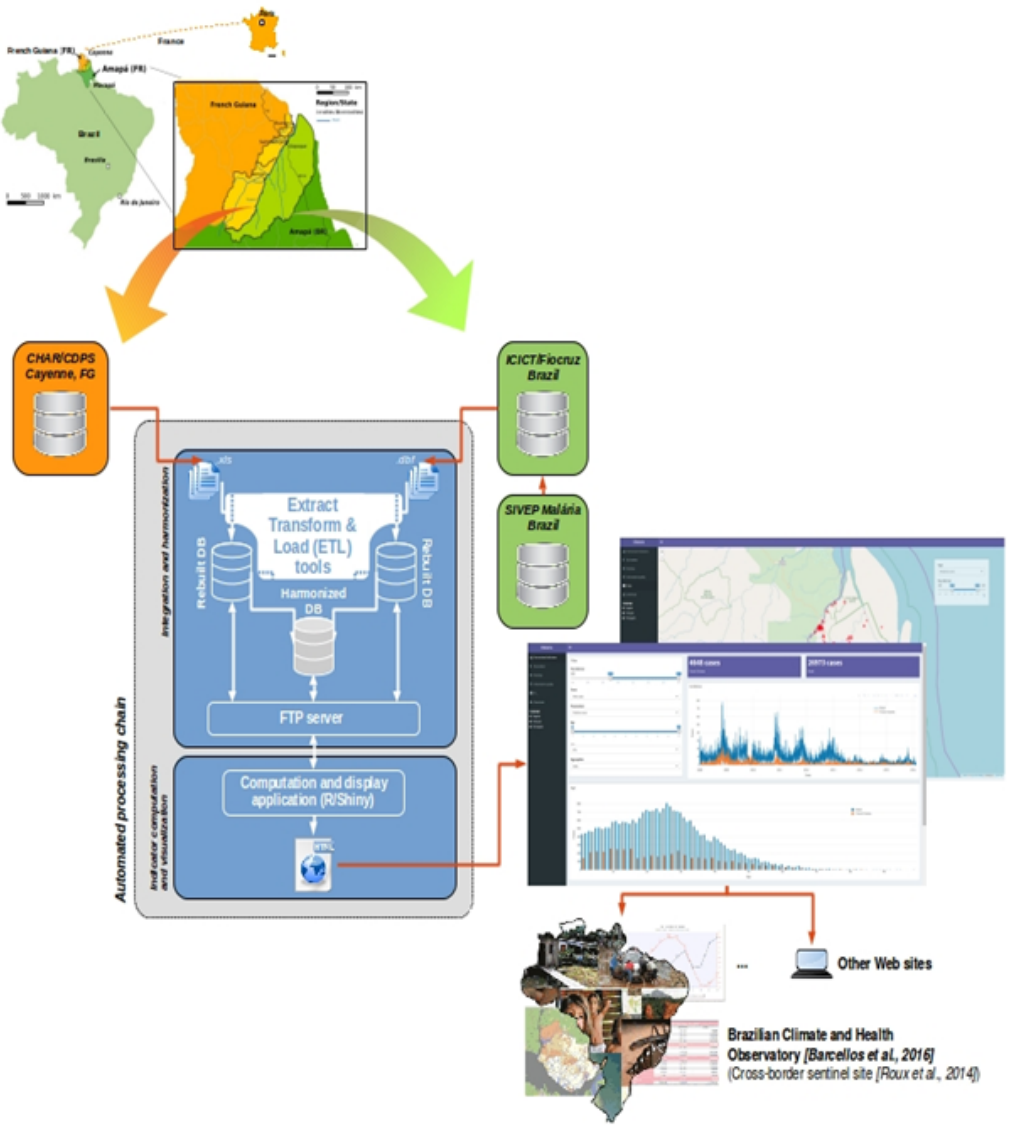

Figure 32: Data flow within the cross-border malaria integration, harmonisation and visualisation system.

mental dynamics, especially for forests, croplands, climate and hydrological resources. Most of these indicators are based on remote sensing data and could thus be applied in other areas in the Amazon. Assessing the robustness of these indicators for other study areas should be an objective for future

researches.

In addition, we showed how some of these indicators can be crossed with socio-economic information in order to derive socio-environmental indicators. These data then need to be better discussed and analyzed with other Work Packages of the project, especially to determine which of them should be automatized in the Observatory web-platform.

5. References

[1] R. Haralick, Statistical and structural approaches to texture, Proceedings of the IEEE 67 (1979) 786–804.

[2] G. W. Frazer, M. A. Wulder, K. O. Niemann, Simulation and quantification of the fine-scale spatial pattern and heterogeneity of forest canopy structure: A lacunarity-based method designed for analysis of continuous canopy heights, Forest Ecology and Management 214 (2005) 65–90.

[3] P. Couteron, Quantifying change in patterned semi-arid vegetation by fourier analysis of digitized aerial photographs, International Journal of Remote Sensing 23 (2002) 3407–3425.

[4] C. Proisy, P. Couteron, F. Fromard, Predicting and mapping mangrove biomass from canopy grain analysis using fourier-based textural ordination of IKONOS images, Remote Sensing of Environment 109 (2007) 379–392.

[5] P. Couteron, N. Barbier, D. Gautier, Textural ordination based on fourier spectral decomposition: A method to analyze and compare landscape patterns, Landscape Ecology 21 (2006) 555–567.

[6] P. Couteron, R. Pelissier, E. A. Nicolini, D. Paget, Predicting tropical forest stand structure parameters from fourier transform of very high-resolution remotely sensed canopy images, Journal of Applied Ecology 42 (2005) 1121–1128.

[7] P. Bugnicourt, S. Guitet, V. F. Santos, L. Blanc, E. D. Sotta, N. Barbier, P. Couteron, Using textural analysis for regional landform and landscape mapping, eastern guiana shield, Geomorphology 317 (2018) 23–44.

[8] Y. Malhi, R. M. Román-Cuesta, Analysis of lacunarity and scales of spatial homogeneity in IKONOS images of amazonian tropical forest canopies, Remote Sensing of Environment 112 (2008) 2074–2087.

[9] M. Palace, M. Keller, G. P. Asner, S. Hagen, B. Braswell, Amazon forest structure from IKONOS satellite data and the automated characterization of forest canopy properties, Biotropica 40 (2007) 141–150.

[10] N. Barbier, P. Couteron, C. Proisy, Y. Malhi, J.-P. Gastellu-Etchegorry, The variation of apparent crown size and canopy heterogeneity across lowland amazonian forests, Global Ecology and Biogeography 19 (2009) 72–84.

[11] P. Ploton, R. Pélissier, C. Proisy, T. Flavenot, N. Barbier, S. N. Rai, P. Couteron, Assessing aboveground tropical forest biomass using google earth canopy images, Ecological Applications 22 (2012) 993–1003.

[12] M. Singh, Y. Malhi, S. Bhagwat, Biomass estimation of mixed forest landscape using a fourier transform texture-based approach on very-high-resolution optical satellite imagery, International Journal of Remote Sensing 35 (2014) 3331–3349.

[13] M. Singh, D. Evans, D. Friess, B. Tan, C. Nin, Mapping above-ground biomass in a tropical forest in cambodia using canopy textures derived from google earth, Remote Sensing 7 (2015) 5057–5076.

[14] S. Pargal, R. Fararoda, G. Rajashekar, N. Balachandran, M. Réjou-Méchain, N. Barbier, C. Jha, R. Pélissier, V. Dadhwal, P. Couteron, Inverting aboveground biomass–canopy texture relationships in a landscape of forest mosaic in the western ghats of india using very high resolution cartosat imagery, Remote Sensing 9 (2017) 228.

[15] N. Barbier, P. Couteron, Attenuating the bidirectional texture variation of satellite images of tropical forest canopies, Remote Sensing of Environment 171 (2015) 245–260.

[16] S. Meng, Y. Pang, Z. Zhang, W. Jia, Z. Li, Mapping aboveground biomass using texture indices from aerial photos in a temperate forest of northeastern china, Remote Sensing 8 (2016) 230.

[17] P. Ploton, N. Barbier, P. Couteron, C. Antin, N. Ayyappan, N. Balachandran, N. Barathan, J.-F. Bastin, G. Chuyong, G. Dauby, V. Droissart, J.-P. Gastellu-Etchegorry, N. Kamdem, D. Kenfack, M. Libalah, G. Mofack, S. Momo, S. Pargal, P. Petronelli, C. Proisy, M. Réjou-Méchain, B. Sonké, N. Texier, D. Thomas, P. Verley, D. Z. Dongmo, U. Berger, R. Pélissier, Toward a general tropical forest biomass prediction model from very high resolution optical satellite images, Remote Sensing of Environment 200 (2017) 140–153.

[18] G. Vincent, D. Sabatier, L. Blanc, J. Chave, E. Weissenbacher, R. Pélissier, E. Fonty, J.-F. Molino, P. Couteron, Accuracy of small footprint airborne LiDAR in its predictions of tropical moist forest stand structure, Remote Sensing of Environment 125 (2012) 23–33.

[19] G. Vincent, D. Sabatier, E. Rutishauser, Revisiting a universal airborne light detection and ranging approach for tropical forest carbon mapping: scaling-up from tree to stand to landscape, Oecologia 175 (2014) 439–443.

[20] G. Bucini, E. F. Lambin, Fire impacts on vegetation in central africa: a remote-sensing-based statistical analysis, Applied Geography 22 (2002) 27–48.

[21] G. Daldegan, O. de Carvalho, R. Guimarães, R. Gomes, F. Ribeiro, C. McManus, Spatial patterns of fire recurrence using remote sensing and GIS in the brazilian savanna: Serra do tombador nature reserve, brazil, Remote Sensing 6 (2014) 9873–9894.

[22] D. C. Morton, R. S. DeFries, J. Nagol, C. M. Souza, E. S. Kasischke, G. C. Hurtt, R. Dubayah, Mapping canopy damage from understory fires in amazon forests using annual time series of landsat and MODIS data, Remote Sensing of Environment 115 (2011) 1706–1720.

[23] L. Giglio, T. Loboda, D. P. Roy, B. Quayle, C. O. Justice, An active-fire based burned area mapping algorithm for the MODIS sensor, Remote Sensing of Environment 113 (2009) 408–420.

[24] A. K. Jain, Global estimation of CO emissions using three sets of satellite data for burned area, Atmospheric Environment 41 (2007) 6931–6940.

[25] S. Silva, L. Vanneschi, A. I. Cabral, M. J. Vasconcelos, A semi-supervised genetic programming method for dealing with noisy labels and hidden overfitting, Swarm and Evolutionary Computation 39 (2018) 323–338.

[26] A. I. Cabral, S. Silva, P. C. Silva, L. Vanneschi, M. J. Vasconcelos, Burned area estimations derived from landsat ETM and OLI data: Comparing genetic programming with maximum likelihood and classification and regression trees, ISPRS Journal of Photogrammetry and Remote Sensing 142 (2018) 94–105.

[27] P. A. Matson, Agricultural intensification and ecosystem properties, Science 277 (1997) 504–509.

[28] D. Tilman, Global environmental impacts of agricultural expansion: The need for sustainable and efficient practices, Proceedings of the National Academy of Sciences 96 (1999) 5995–6000.

[29] K. G. Cassman, Ecological intensification of cereal production systems: Yield potential, soil quality, and precision agriculture, Proceedings of the National Academy of Sciences 96 (1999) 5952–5959.

[30] D. Arvor, M. Jonathan, M. S. P. Meirelles, V. Dubreuil, L. Durieux, Classification of MODIS EVI time series for crop mapping in the state of mato grosso, brazil, International Journal of Remote Sensing 32 (2011) 7847–7871.

[31] S. S. Ray, A. Sood, S. Panigrahy, J. S. Parihar, Derivation of indices using remote sensing data to evaluate cropping systems, Journal of the Indian Society of Remote Sensing 33 (2005) 475–481.

[32] D. Arvor, I. Tritsch, C. Barcellos, N. Jégou, V. Dubreuil, Land use sustainability on the south-eastern amazon agricultural frontier: Recent progress and the challenges ahead, Applied Geography 80 (2017) 86 – 97.

[33] C. Neill, M. T. Coe, S. H. Riskin, A. V. Krusche, H. Elsenbeer, M. N. Macedo, R. McHorney, P. Lefebvre, E. A. Davidson, R. Scheffler, A. M. e. S. Figueira, S. Porder, L. A. Deegan, Watershed responses to amazon

soya bean cropland expansion and intensification, Philosophical Transactions of the Royal Society B: Biological Sciences 368 (????) 20120425–20120425.

[34] P. M. Fearnside, Soybean cultivation as a threat to the environment in Brazil, Environmental Conservation (2001) 23–38.

[35] P. M. Fearnside, Dams in the amazon: Belo monte and brazils hydroelectric development of the xingu river basin, Environmental Management 38 (2006) 16–27.

[36] E. M. Latrubesse, E. Y. Arima, T. Dunne, E. Park, V. R. Baker, F. M. dHorta, C. Wight, F. Wittmann, J. Zuanon, P. A. Baker, C. C. Ribas, R. B. Norgaard, N. Filizola, A. Ansar, B. Flyvbjerg, J. C. Stevaux, Damming the rivers of the amazon basin, Nature 546 (2017) 363–369.

[37] S. M. Powers, D. M. Robertson, E. H. Stanley, Effects of lakes and reservoirs on annual river nitrogen, phosphorus, and sediment export in agricultural and forested landscapes: EFFECTS OF LAKES AND RESERVOIRS ON RIVER NUTRIENTS AND SEDIMENT, Hydrological Processes 28 (2014) 5919–5937.

[38] V. J. Santucci, S. R. Gephard, S. M. Pescitelli, Effects of multiple low-head dams on fish, macroinvertebrates, habitat, and water quality in the fox river, illinois, North American Journal of Fisheries Management 25 (2005) 975–992.

[39] F. Habets, E. Philippe, E. Martin, C. H. David, F. Leseur, Small farm dams: impact on river flows and sustainability in a context of climate change, Hydrology and Earth System Sciences 18 (2014) 4207–4222.

[40] J. Callow, K. Smettem, The effect of farm dams and constructed banks on hydrologic connectivity and runoff estimation in agricultural landscapes, Environmental Modelling & Software 24 (2009) 959–968.

[41] V. T. C. Malveira, J. C. de Araújo, A. Güntner, Hydrological impact of a high-density reservoir network in semiarid northeastern brazil, Journal of Hydrologic Engineering 17 (2012) 109–117.

[42] A. Gütner, M. S. Krol, J. C. D. Araújo, A. Bronstert, Simple water balance modelling of surface reservoir systems in a large data-scarce semiarid region / Modlisation simple du bilan hydrologique de systmes de rservoirs de surface dans une grande rgion semi-aride pauvre en donnes, Hydrological Sciences Journal 49 (2004).

[43] B. Lehner, C. R. Liermann, C. Revenga, C. Vrsmarty, B. Fekete, P. Crouzet, P. Dll, M. Endejan, K. Frenken, J. Magome, C. Nilsson, J. C. Robertson, R. Rdel, N. Sindorf, D. Wisser, High-resolution mapping of the world's reservoirs and dams for sustainable river-flow management, Frontiers in Ecology and the Environment 9 (2011) 494–502.

[44] M. J. Deitch, A. M. Merenlender, S. Feirer, Cumulative effects of small reservoirs on streamflow in northern coastal california catchments, Water Resources Management (2013).

[45] D. Arvor, F. R. Daher, D. Briand, S. Dufour, A.-J. Rollet, M. Simões, R. P. Ferraz, Monitoring thirty years of small water reservoirs proliferation in the southern brazilian amazon with landsat time series, ISPRS Journal of Photogrammetry and Remote Sensing (2018).

[46] J. A. Marengo, J. C. Espinoza, Extreme seasonal droughts and floods in Amazonia: causes, trends and impacts: EXTREMES IN AMAZONIA, International Journal of Climatology 36 (2016) 1033–1050.

[47] E. A. Davidson, A. C. de Arajo, P. Artaxo, J. K. Balch, I. F. Brown, M. M. C. Bustamante, M. T. Coe, R. S. DeFries, M. Keller, M. Longo, J. W. Munger, W. Schroeder, B. S. Soares-Filho, C. M. Souza, S. C. Wofsy, The amazon basin in transition, Nature 481 (????) 321–328.

[48] C. A. Nobre, G. Sampaio, L. S. Borma, J. C. Castilla-Rubio, J. S. Silva, M. Cardoso, Land-use and climate change risks in the Amazon and the need of a novel sustainable development paradigm, Proceedings of the National Academy of Sciences 113 (2016) 10759–10768.

[49] B. Liebmann, S. J. Camargo, A. Seth, J. A. Marengo, L. M. V. Carvalho, D. Allured, R. Fu, C. S. Vera, Onset and end of the rainy season in south america in observations and the ECHAM 4.5 atmospheric general circulation model, Journal of Climate 20 (2007) 2037–2050.

[50] J. Khanna, D. Medvigy, S. Fueglistaler, R. Walko, Regional dry-season climate changes due to three decades of amazonian deforestation, Nature Climate Change 7 (2017) 200–204.

[51] R. Fu, L. Yin, W. Li, P. A. Arias, R. E. Dickinson, L. Huang, S. Chakraborty, K. Fernandes, B. Liebmann, R. Fisher, R. B. Myneni, Increased dry-season length over southern amazonia in recent decades and its implication for future climate projection, Proceedings of the National Academy of Sciences 110 (2013) 18110–18115.

[52] D. Arvor, B. Funatsu, V. Michot, V. Dubreuil, Monitoring rainfall patterns in the southern amazon with PERSIANN-CDR data: Long-term characteristics and trends, Remote Sensing 9 (2017) 889.

[53] A. S. L. Rodrigues, R. M. Ewers, L. Parry, C. Souza, A. Veríssimo, A. Balmford, Boom-and-Bust Development Patterns Across the Amazon Deforestation Frontier, Science 324 (2009) 1435–1437.

[54] D. Celentano, E. Sills, M. Sales, A. Veríssimo, Welfare Outcomes and the Advance of the Deforestation Frontier in the Brazilian Amazon, World Development 40 (2012) 850–864.

[55] D. Celentano, A. Veríssimo, The Amazon Frontier Advance: From Boom To Bust, IMAZON, Belém, 2007.

[56] R. R. Sears, C. Padoch, M. Pinedo-Vasquez, Amazon Forestry Tranformed: Integrating Knowledge for Smallholder Timber Managemet in Eastern Brazil, Human Ecology 35 (2007) 697–707.

[57] D. Weinhold, E. J. Reis, P. M. Vale, Boom-bust patterns in the Brazilian Amazon, Global Environmental Change 35 (2015) 391–399.

[58] D. Nepstad, D. McGrath, C. Stickler, A. Alencar, A. Azevedo, B. Swette, T. Bezerra, M. DiGiano, J. Shimada, R. Seroa da Motta, E. Armijo, L. Castello, P. Brando, M. C. Hansen, M. McGrath-Horn, O. Carvalho, L. Hess, Slowing Amazon deforestation through public policy and interventions in beef and soy supply chains, Science 344 (2014) 1118–1123.

[59] E. Y. Arima, P. Barreto, E. Araújo, B. Soares-Filho, Public policies can reduce tropical deforestation: Lessons and challenges from Brazil, Land Use Policy 41 (2014) 465–473.

[60] J. Caviglia-Harris, E. Sills, A. Bell, D. Harris, K. Mullan, D. Roberts, Busting the Boom–Bust Pattern of Development in the Brazilian Amazon, World Development 79 (2016) 82–96.

[61] S. Dinda, Environmental Kuznets Curve Hypothesis: A Survey, Ecological Economics 49 (2004) 431–455.

[62] A. Pfaff, R. Walker, Regional interdependence and forest transitions: Substitute deforestation limits the relevance of local reversals, Land Use Policy 27 (2010) 119–129.

[63] IBGE, Censos demográficos, 2010.

[64] INPE, Metodologia para o Cálculo da Taxa Anual de Desmatamento na Amazônia Legal., Technical Report, 2014.

[65] I. Tritsch, D. Arvor, Transition in environmental governance in the Brazilian Amazon: emergence of a new pattern of socio-economic development and deforestation, Land Use Policy 59 (2016) 446–455.

[66] J. Choumert, P. Combes Motel, H. K. Dakpo, Is the Environmental Kuznets Curve for deforestation a threatened theory? A meta-analysis of the literature, Ecological Economics 90 (2013) 19–28.

[67] A.-E. Laques, A. I. R. Cabral, S. C. P. da Silva, H. D. S. Pereira, C. H. Saito, Água e floresta na reserva de desenvolvimento sustentável do uatumã, Sustentabilidade em Debate 9 (2018) 164.

[68] G. L. Galford, B. Soares-Filho, C. E. P. Cerri, Prospects for land-use sustainability on the agricultural frontier of the Brazilian Amazon, Philosophical Transactions of the Royal Society B: Biological Sciences 368 (2013) 20120171–20120171.

[69] D. M. Lapola, L. A. Martinelli, C. A. Peres, J. P. H. B. Ometto, M. E. Ferreira, C. A. Nobre, A. P. D. Aguiar, M. M. C. Bustamante, M. F. Cardoso, M. H. Costa, C. A. Joly, C. C. Leite, P. Moutinho, G. Sampaio, B. B. N. Strassburg, I. C. G. Vieira, Pervasive transition of the Brazilian land-use system, Nature Climate Change 4 (2014) 27–35. WOS:000333666600012.

[70] D. Arvor, V. Dubreuil, P. Mendez, C. M. Ferreira, M. Meirelles, Développement, crises et adaptation des territoires du soja au Mato Grosso: l'exemple de Sorriso, Confins (2009).

[71] D. Arvor, I. Tritsch, C. Barcellos, N. Jégou, V. Dubreuil, Land use sustainability on the south-eastern amazon agricultural frontier: Recent progress and the challenges ahead, Applied Geography 80 (2017) 86–97.

[72] J. Hansen, M. Sato, R. Ruedy, Perception of climate change, Proceedings of the National Academy of Sciences 109 (2012) E2415–E2423.

[73] V. Dubreuil, B. M. Funatsu, V. Michot, S. Nasuti, N. Debortoli, N. A. de Mello-Thery, F.-M. L. Tourneau, Local rainfall trends and their perceptions by amazonian communities, Climatic Change 143 (2017) 461–472.

[74] A. Stefani, I. Dusfour, A. P. S. Corrêa, M. C. Cruz, N. Dessay, A. K. Galardo, C. D. Galardo, R. Girod, M. S. Gomes, H. Gurgel, A. C. F. Lima, E. S. Moreno, L. Musset, M. Nacher, A. C. Soares, B. Carme, E. Roux, Land cover, land use and malaria in the amazon: a systematic literature review of studies using remotely sensed data, Malaria Journal 12 (2013) 192.

[75] A. Stefani, E. Roux, J.-M. Fotsing, B. Carme, Studying relationships between environment and malaria incidence in camopi (french guiana) through the objective selection of buffer-based landscape characterisations, International Journal of Health Geographics 10 (2011) 65.

[76] Z. Li, E. Roux, N. Dessay, R. Girod, A. Stefani, M. Nacher, A. Moiret, F. Seyler, Mapping a knowledge-based malaria hazard index related to landscape using remote sensing: Application to the cross-border area between french guiana and brazil, Remote Sensing 8 (2016) 319.

[77] Z. Li, T. Catry, N. Dessay, H. da Costa Gurgel, C. A. de Almeida, C. Barcellos, E. Roux, Regionalization of a landscape-based hazard index of malaria transmission: An example of the state of amapá, brazil, Data 2 (2017) 37.

[78] E. Roux, R. F. Saldanha, Christovam Barcellos, T. Mandon, M. Gomes, E. Mosnier, B. Guarmit, Jean-Christophe Desconnets, Cross-border epi-

demiological data integration and harmonization application to malaria in the cross-border area between french guiana and brazil (2018).